International Journal of Solids and Structures 49 (2012) 3008–3021

Contents lists available at SciVerse ScienceDirect

International Journal of Solids and Structures

journal homepage: www.elsevier.com/locate/ijsolstr

A mode III crack crossing the magnetoelectroelastic bimaterial interface under concentrated magnetoelectromechanical loads

Yongping Wan *, Yanpeng Yue, Zheng Zhong

School of Aerospace Engineering and Applied Mechanics, Tongji University, Shanghai 200092, PR China

ARTICLE INFO

Article history:
Received 3 March 2012
Received in revised form 8 May 2012
Available online 13 June 2012

Keywords:
Dissimilar magnetoelectroelastic bimaterial
Crack cutting interface
Green's function

ABSTRACT

A mode III crack cutting perpendicularly across the interface between two dissimilar semi-infinite magnetoelectroelastic solid is studied under the combined loads of a line force, a line electric charge and a line magnetic charge at an arbitrary location. The impermeable conditions are implied on the crack faces. The technique developed in literature for the elastic bimaterial with a crack cutting interface is exploited to treat the magnetoelectroelastic bimaterial. The Riemann-Hilbert problem can be formulated and solved based on complex variable method. Analytical solutions can be obtained for the entire plane. The intensity factors around crack tips can be defined for the elastic, electric and magnetic fields. It shows that, no matter where the load position is, the electric displacement intensity factors (EDIFs), as well as the magnetic induction intensity factors (MIIFs), are identical in magnitude but opposite in sign for both crack tips, on condition that a line force is solely applied. Alternatively, if only a line electric charge is considered, then the stress intensity factors (SIFs) and the MIIFs exhibit the behavior. Likewise, if only a line magnetic charge is applied, it turns to the SIFs and the EDIFs instead. In addition, the dependence of the intensity factors is graphically shown with respect to the location of a line force. It is found that the SIF for a crack tip tends to be infinite if the applied force is approaching the tip itself, but the EDIF, with the complete opposite trend, tends to be vanishing. Finally, focusing on the more practical case of piezoelectric/piezomagnetic bimaterial, variation of the SIF along with the moduli as well as the piezo constitutive coefficients is explored. These analyses may provide some guidance for material selection by minimizing the SIF. It is also believed that the results obtained in this paper can serve as the Green's function for the dissimilar magnetoelectroelastic semi-infinite bimaterial with a crack cutting the interface under general magnetoelectromechanical loads.

1. Introduction

Piezoelectric and piezomagnetic composite are nowadays used to fabricate the magnetoelectroelastic solids, where mechanical, electric and magnetic coupling can be achieved. The product property of magnetoelectric coupling effect can be much pronounced than the intrinsic magnetoelectric coefficient present in few natural materials. Therefore, magnetoelectroelastic solids have been studied with remarkable interests in recent years, due to the great potential applications in smart sensors, transducers and other new technology. Since the magnetoelectric coupling can be much higher in layered structures than other configuration, the layered piezoelectric and piezomagnetic composite becomes the top priori in the design of the magnetoelectroelastic composite, where distinct interface usually exists. On the other hand, crack-like flaws are inevitably present around the interface in the manufacturing process or during the service of piezoelectric/piezomagnetic composite materials. Thus, analysis of cracks interacting with interface in magnetoelectroelastic material is necessary.

For the crack analysis of magnetoelectroelastic solids with bimaterial interface, Gao et al. (2003) presented an explicitly analytic solution for a magnetoelectrically permeable interface crack between two dissimilar magnetoelectroelastic solids for the generalized 2-dimensional problem. Soh and Liu (2004) have solved the half-plane composed of two dissimilar magetoelectroelastic solids with an interface edge crack under anti-plane deformation. The electrically and magnetically impermeable conditions are adopted on the free surfaces of the half plane as well as the crack faces. Zhou et al. (2005) solved by Schmidt method the problem of two bonded dissimilar magnetoelectroelastic half-planes with collinear interface cracks under a harmonic anti-plane shear impact, where electrically and magnetically permeable conditions are adopted on the crack surfaces. Tian and Gabbert (2005) adopted the continuously distributed edge dislocations to model a parallel crack near the bimaterial interface of two magnetoelectroelastic half-plane. Li and Kardomateas (2006) investigated the mode III interface crack problem between dissimilar piezo-electromagneto-elastic

* Corresponding author.
E-mail address: wanyp@tongji.edu.cn (Y. Wan).

0020-7683/$ - see front matter © 2012 Elsevier Ltd. All rights reserved.
http://dx.doi.org/10.1016/j.ijsolstr.2012.06.001

bimaterials, taking the electromagnetic field inside the crack into account. Closed form solutions are derived for impermeable and permeable cracks. Furthermore, they (Li and Kardomateas, 2007) also studied the in-plane problem, where additional types of oscillating singularities were found for the piezoelectroelastic field around crack tip, compared to the solutions for dissimilar elastic bimaterial or piezoelectric bimaterials. Wang and Mai (2006) solved the antiplane mechanical and in-plane electric and magnetic fields for an interface crack between two dissimilar magneto-electroelastic layers of finite thickness. By using Fourier transform method, Hu et al. (2006) and Zhong and Li (2006) solved the problem of an anti-plane Yoffe-type interface crack moving with a constant speed along the interface between two semi-infinite magnetoelectroelastic materials. Su and Feng (2008) used the finite Fourier transform method to solve the anti-plane interface crack between two dissimilar magnetoelectroelastic plates, subjected to anti-plane mechanical and in-plane magneto-electrical loads, where the interface crack is assumed to be either magneto-electrically impermeable or permeable, and the position of the interface crack can be arbitrary. By using the integral transform and Cauchy singular integral equation methods (Feng et al., 2009), the dynamic response of an interfacial crack between two dissimilar magneto-electroelastic layers of finite thickness is investigated under magnetoelectromechanical impact loads on crack face. Also, Feng et al. (2010) investigated multiple interfacial cracks between two dissimilar magnetoelectroelastic layers of finite width subjected to in-plane magnetoelectromechanical loads, where the crack surfaces are assumed to be magnetoelectrically impermeable. In addition, the contact zone model has also been introduced into the analysis for crack interacting with interface in magnetoelectroelastic bimaterials. Herrmann et al. (2010) considered an interface crack with a frictionless contact zone at the right crack tip between two semi-infinite piezoelectric/piezomagnetic spaces under the action of the planar remote mechanical load, magnetic and electric fluxes as well as concentrated forces at the crack faces, where two kinds of magnetoelectrical boundary conditions at the crack faces, i.e., magnetoelectrically permeable, magnetically impermeable and electrically permeable, were considered. Feng et al. (2011) studied an interface crack with a frictionless contact zone at the right crack-tip between two dissimilar magnetoelectroelastic materials under the action of concentrated magnetoelectromechanical loads on the crack faces. The open part of the crack is assumed to be magnetically impermeable and electrically permeable.

It is known cracks easily initiate nearby interface in composite. Previous studies mainly focus on the cracks lying on interface. However, there may exist diverse configurations of crack in magnetoelectroelastic solids. Li and Lee (2008) analyze an anti-plane crack perpendicularly intersecting the interface of two dissimilar graded magnetoelectroelastic infinite strips. The impermeable electromagnetic conditions are adopted on the crack faces. Li et al. (2009) considered the anti-plane shear crack perpendicular to and terminating at the interface of the bimagnetoelectric semi-infinite solid. On the crack faces, a constant shear stress is exerted, and the magnetic and electric permeable conditions are adopted. In addition to the crack terminating at the interface, cracks may also propagate across the interface of magnetoelectroelastic bimaterials. In this paper, we pay attention to the crack cutting perpendicularly across the bimaterial interface of dissimilar magnetoelectroelastic solids. For the through crack crossing the interface of two transversely orthotropic magnetoelectroelastic materials under longitudinal shear and inplane electric and magnetic loads, the antiplane deformation prevails. Only the out-of-plane displacement is coupled to the in-plane electric and magnetic fields. The problem with a crack vertically crossing the elastic bimaterial interface has been addressed by Xiao and Xie (2008), where the complex variable method was used to find the analytical solution. In this paper, the anti-plane crack cutting perpendicularly across the bimaterial interface of two semi-infinite magnetoelectroelastic solids was studied under the combined loads of a line force, a line electric charge and a line magnetic charge. The technique developed in Xiao and Xie (2008) will be used. In the mapping plane, the mode III interface crack between dissimilar semi-infinite magnetoelectroelastic planes was solved by using the complex variable method. On the crack face, the impermeable conditions, i.e., electrically and magnetically impermeable, are adopted. The combined line magnetoelectromechanical loads are assumed at an arbitrary point in the upper semi-infinite plane. The Riemann-Hilbert problem can be formulated and solved based on complex variable method. Analytical solutions can be obtained for the entire plane and accordingly, the intensity factors around crack tips can be defined for the mechanical, electric and magnetic fields. The obtained results in this paper include as special cases the elastic bimaterial with a crack cutting across interface, the mode III crack in an infinite homogeneous magnetoelectroelastic, piezoelectric or piezomagnetic materials. It is shown that, when the combined loads reduce to a line force, the electric displacement intensity factors (EDIFs), as well as the magnetic induction intensity factors (MIIFs), are identical in magnitude but opposite in sign for both crack tips, no matter where the load position is. Alternatively, if only a line electric charge is considered, then the stress intensity factors (SIFs) and the MIIFs exhibit the behavior. Likewise, if a line magnetic charge is solely applied, then it turns to the SIFs and the EDIFs instead. In addition, the dependence of the intensity factors is graphically shown with respect to the location of a line force. It is found that the SIF for a crack tip tends to be infinite if the applied force is approaching the tip itself, but the EDIF, with the complete opposite trend, tends to be vanishing. Finally, focusing on the more practical case of piezoelectric/piezomagnetic bimaterial, variation of the SIF along with the moduli as well as the piezo constitutive coefficients is explored.

2. Problem formulation

Schematically illustrated in Fig. 1(a) is the dissimilar magneto-electroelastic bimaterial with a crack perpendicularly cutting across the interface. Two different magnetoelectroelastic materials respectively occupy the upper and the lower half planes, which are denoted respectively by the superscripts I and II hereafter. The bimaterial interface is cut by a crack of length $2a$ into two parts, l_1 and l_2. The crack lies symmetrically across the interface, with the same length a in the upper and lower half plane. The coordinates are placed as shown in Fig. 1(a), where the x_2 axis coincides with the crack, l_1 and l_2 lie on the negative and positive part of the x_1 axis, respectively. The crack tips are respectively denoted by A and C with the coordinates $(0,a)$ and $(0,-a)$. The crack face interacts with l_1 and l_2 at $B(0^-,0)$ and $D(0^+,0)$. The plane incorporating the x_1 and x_2 axes can be denoted as the $z=x_1+ix_2$ plane, where $i=\sqrt{-1}$. We consider a concentrated magnetoelectromechanical load $(\sigma_3, q_{e0}, q_{m0})$ applied at an arbitrary location z_0. The combined loads are composed of a line force σ_3 vertical to the z plane, a line electric charge q_{e0} and a line magnetic charge q_{m0}. In this paper, without loss of any generality, z_0 is assumed to be in the upper half-plane. The magnetoelectroelastic conditions on the bimaterial interface are as follows,

$$\gamma_{31}^{I}(x_1,0)=\gamma_{31}^{II}(x_1,0),\quad \tau_{32}^{I}(x_1,0)=\tau_{32}^{II}(x_1,0),\quad x_1\in(-\infty,\infty) \quad (1a,b)$$

$$D_2^{I}(x_1,0)=D_2^{II}(x_1,0),\quad E_1^{I}(x_1,0)=E_1^{II}(x_1,0),\quad x_1\in(-\infty,\infty) \quad (2a,b)$$

$$B_2^{I}(x_1,0)=B_2^{II}(x_1,0),\quad H_1^{I}(x_1,0)=H_1^{II}(x_1,0),\quad x_1\in(-\infty,\infty) \quad (3a,b)$$

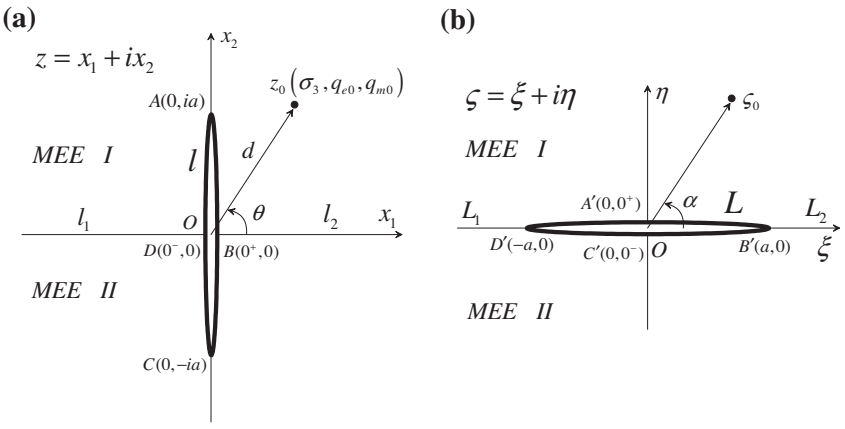

Fig. 1. A mode III crack cutting across the interface of dissimilar semi-infinite magnetoelectroelastic planes (a) the physical plane (b) the mapping plane.

where γ and τ are shear strain and shear stress, D and E are the electric displacement and electric field, B and H are magnetic induction and magnetic field. The subscripts 1 and 2 represent the components along x_1 and x_2 axes respectively. The crack faces are tractions free. Different electromagnetic conditions on crack face exist in literature, including the permeable, impermeable conditions, etc. We just consider in this paper the electrically and magnetically impermeable conditions on the crack surface, i.e.,

$$\tau_{31}^k(0^+, x_2) = \tau_{31}^k(0^-, x_2) = 0 \tag{4a, b}$$

$$D_1^k(0^+, x_2) = D_1^k(0^-, x_2) = 0 \tag{5a, b}$$

$$B_1^k(0^+, x_2) = B_1^k(0^-, x_2) = 0 \tag{6a, b}$$

In Eqs. (4)–(6), $x_2 \in (0, a)$ when $k = I$, or $x_2 \in (-a, 0)$ when $k = II$. Denote w^k, ϕ^k, φ^k as the mechanical displacements, the electric potentials and the magnetic potentials, respectively, which can generally be expressed as,

$$w^k(x_1, x_2) = 2Im\left[U^k(z)\right] \tag{7a}$$

$$\phi^k(x_1, x_2) = 2Im\left[\Phi^k(z)\right] \tag{7b}$$

$$\varphi^k(x_1, x_2) = 2Im\left[\Psi^k(z)\right] \tag{7c}$$

where $Im[\bullet]$ represent the imaginary part. $U^k(z), \Phi^k(z), \Psi^k(z)$ are analytical functions given by,

$$U^k(z) = p_1\delta_{1k}\ln(z - z_0) + U_0^k(z) \tag{8a}$$

$$\Phi^k(z) = p_2\delta_{1k}\ln(z - z_0) + \Phi_0^k(z) \tag{8b}$$

$$\Psi^k(z) = p_3\delta_{1k}\ln(z - z_0) + \Psi_0^k(z) \tag{8c}$$

in which δ_{1k} is the Kronecker Delta, $p_j (j = 1, 2, 3)$ are constants to be determined. $U_0^k(z), \Phi_0^k(z), \Psi_0^k(z)$ are analytical functions on the entire plane except the crack, which vanish in the infinity, i.e.,

$$U_0^k(\infty) = \Phi_0^k(\infty) = \Psi_0^k(\infty) = 0 \tag{9}$$

The extended gradient equations and constitutive equations can be given by,

$$E_2^k + iE_1^k = -2\phi^k(z), \quad H_2^k + iH_1^k = -2\psi^k(z),$$
$$\gamma_{32}^k + i\gamma_{31}^k = 2u^k(z) \quad (10a, b, c) \tag{10a, b, c}$$

$$\tau_{32}^k + i\tau_{31}^k = 2\left[C_{44}^k u^k(z) + e_{15}^k\phi^k(z) + h_{15}^k\psi^k(z)\right] \tag{11a}$$

$$D_2^k + iD_1^k = 2\left[e_{15}^k u^k(z) - \varepsilon_{11}^k\phi^k(z) - \beta_{11}^k\psi^k(z)\right] \tag{11b}$$

$$B_2^k + iB_1^k = 2\left[h_{15}^k u^k(z) - \beta_{11}^k\phi^k(z) - \mu_{11}^k\psi^k(z)\right] \tag{11c}$$

where C_{44}^k are the shear moduli, e_{15}^k the piezoelectric coefficients, h_{15}^k the piezomagnetic coefficients, ε_{11}^k the dielectric permittivities, β_{11}^k the magnetoelectric coefficients, μ_{11}^k the magnetic permeabilities.

$$u^k(z) = \frac{p_1\delta_{1k}}{z - z_0} + u_0^k(z) \tag{12a}$$

$$\phi^k(z) = \frac{p_2\delta_{1k}}{z - z_0} + \phi_0^k(z) \tag{12b}$$

$$\psi^k(z) = \frac{p_3\delta_{1k}}{z - z_0} + \psi_0^k(z) \tag{12c}$$

$$u_0^k(z) = \frac{d}{dz}U_0^k(z), \quad \phi_0^k(z) = \frac{d}{dz}\Phi_0^k(z), \quad \psi_0^k(z) = \frac{d}{dz}\Psi_0^k(z) \tag{13a, b, c}$$

In terms of Gaussian theorem for concentrated magnetic and electric loads, and also the mechanical equilibrium around the line force, the following equations can be established,

$$C_{44}^I p_1 + e_{15}^I p_2 + h_{15}^I p_3 = -\frac{\sigma_3}{4\pi i} \tag{14a}$$

$$e_{15}^I p_1 - \varepsilon_{11}^I p_2 - \beta_{11}^I p_3 = -\frac{q_{e0}}{4\pi i} \tag{14b}$$

$$h_{15}^I p_1 - \beta_{11}^I p_2 - \mu_{11}^I p_3 = -\frac{q_{m0}}{4\pi i} \tag{14c}$$

from which p_1, p_2, p_3 can be derived as

$$p_1 = -\frac{1}{4\pi i\rho}\left[\left(\varepsilon_{11}^I\mu_{11}^I - (\beta_{11}^I)^2\right)\sigma_3 + \left(e_{15}^I\mu_{11}^I - h_{15}^I\beta_{11}^I\right)q_{e0} + \left(h_{15}^I\varepsilon_{11}^I - e_{15}^I\beta_{11}^I\right)q_{m0}\right] \tag{15a}$$

$$p_2 = -\frac{1}{4\pi i\rho}\left[\left(e_{15}^I\mu_{11}^I - h_{15}^I\beta_{11}^I\right)\sigma_3 - \left(\left(h_{15}^I\right)^2 + C_{44}^I\mu_{11}^I\right)q_{e0} + \left(e_{15}^I h_{15}^I + C_{44}^I\beta_{11}^I\right)q_{m0}\right] \tag{15b}$$

$$p_3 = -\frac{1}{4\pi i\rho}\left[\left(h_{15}^I\varepsilon_{11}^I - e_{15}^I\beta_{11}^I\right)\sigma_3 + \left(e_{15}^I h_{15}^I + C_{44}^I\beta_{11}^I\right)q_{e0} - \left((e_{15}^I)^2 + C_{44}^I\varepsilon_{11}^I\right)q_{m0}\right] \tag{15c}$$

where

$$\rho = \left(h_{15}^I\right)^2\varepsilon_{11}^I + (e_{15}^I)^2\mu_{11}^I + C_{44}^I\varepsilon_{11}^I\mu_{11}^I - 2e_{15}^I h_{15}^I\beta_{11}^I - C_{44}^I(\beta_{11}^I)^2 \tag{16}$$

Inserting Eq. (12) and (13) into Eq. (10) and (11), and noticing Eq. (14), the magnetoelectroelastic fields in complex formulation can be obtained (Appendix A).

We seek to find the analytical solution of a crack cutting across the interface in the mapping plane. Similar to Xiao and Xie (2008), the following conformal mapping function is adopted,

$$z = \omega(\varsigma) = \sqrt{\varsigma^2 - a^2} \tag{17}$$

where $\varsigma = \xi + i\eta$, as shown in Fig. 1(b). By using Eq. (17), the upper and lower half-planes of the z plane are transformed respectively into the upper and lower half-planes of the ς plane. The crack face, denoted as $l(ABCDA)$ and lying on the imaginary axis in z plane, is

mapped into $L(A'B'C'D'A')$ which now lies on the real axis in the ς plane. The interface l_1 and l_2 are transformed respectively into L_1 and L_2, which also lie on the real axis in the ς plane. The imaginary axis outside the crack in the z plane, i.e., the parts with $x_2 > a$ and $x_2 < -a$, are mapped respectively to the positive and negative parts of the imaginary axis in ς plane. Accordingly, the load position z_0 is transformed to $\varsigma_0 = \sqrt{z_0^2 + a^2}$.

We now formulate the problem in the mapping plane. The magnetoelectroelastic fields listed in Appendix A should now be transformed into the ς plane. The following Taylor series expansion in the vicinity of ς_0 on the mapping plane is adopted.

$$\frac{1}{z-z_0} = \frac{1}{\varsigma-\varsigma_0}\frac{\sqrt{\varsigma^2-a^2}+\sqrt{\varsigma_0^2-a^2}}{\varsigma+\varsigma_0} = \frac{1}{\varsigma-\varsigma_0}\left[\frac{z_0}{\varsigma_0} + \Theta_1(\varsigma-\varsigma_0) + \Theta_2(\varsigma-\varsigma_0)^2 + \cdots\right] \tag{18}$$

where $\Theta_i (i = 1, 2\ldots)$ are the expansion coefficients. Denote that $\Omega(\varsigma) = \Theta_1 + \Theta_2(\varsigma-\varsigma_0) + \cdots$. Then Eq. (18) becomes

$$\frac{1}{z-z_0} = \frac{1}{\varsigma-\varsigma_0}\frac{z_0}{\varsigma_0} + \Omega(\varsigma) \tag{19}$$

where $\Omega(\varsigma)$ can be taken as an unknown analytic function on the entire plane except for several isolated singular points. Inserting Eq. (19) into Eqs. (A.1)–(A.3) and (A.7)–(A.9), the magnetoelectroelastic fields can be formulated in the mapping plane as follows,

$$\tau_{32}^I + i\tau_{31}^I = 2\left[-\frac{\sigma_3}{4\pi i}\frac{z_0}{\varsigma_0}\frac{1}{\varsigma-\varsigma_0} + C_{44}^I u_0^{I*}(\varsigma) + e_{15}^I\phi_0^{I*}(\varsigma) + h_{15}^I\psi_0^{I*}(\varsigma)\right] \tag{20a}$$

$$D_2^I + iD_1^I = 2\left[-\frac{q_{e0}}{4\pi i}\frac{z_0}{\varsigma_0}\frac{1}{\varsigma-\varsigma_0} + e_{15}^I u_0^{I*}(\varsigma) - \varepsilon_{11}^I\phi_0^{I*}(\varsigma) - \beta_{11}^I\psi_0^{I*}(\varsigma)\right] \tag{20b}$$

$$B_2^I + iB_1^I = 2\left[-\frac{q_{m0}}{4\pi i}\frac{z_0}{\varsigma_0}\frac{1}{\varsigma-\varsigma_0} + h_{15}^I u_0^{I*}(\varsigma) - \beta_{11}^I\phi_0^{I*}(\varsigma) - \mu_{11}^I\psi_0^{I*}(\varsigma)\right] \tag{20c}$$

$$\tau_{32}^{II} + i\tau_{31}^{II} = 2\left[C_{44}^{II} u_0^{II*}(\varsigma) + e_{15}^{II}\phi_0^{II*}(\varsigma) + h_{15}^{II}\psi_0^{II*}(\varsigma)\right] \tag{21a}$$

$$D_2^{II} + iD_1^{II} = 2\left[e_{15}^{II} u_0^{II*}(\varsigma) - \varepsilon_{11}^{II}\phi_0^{II*}(\varsigma) - \beta_{11}^{II}\psi_0^{II*}(\varsigma)\right] \tag{21b}$$

$$B_2^{II} + iB_1^{II} = 2\left[h_{15}^{II} u_0^{II*}(\varsigma) - \beta_{11}^{II}\phi_0^{II*}(\varsigma) - \mu_{11}^{II}\psi_0^{II*}(\varsigma)\right] \tag{21c}$$

$$\gamma_{32}^I + i\gamma_{31}^I = 2\left[\frac{z_0}{\varsigma_0}\frac{p_1}{\varsigma-\varsigma_0} + u_0^{I*}(\varsigma)\right] \tag{22a}$$

$$E_2^I + iE_1^I = -2\left[\frac{z_0}{\varsigma_0}\frac{p_2}{\varsigma-\varsigma_0} + \phi_0^{I*}(\varsigma)\right] \tag{22b}$$

$$H_2^I + iH_1^I = -2\left[\frac{z_0}{\varsigma_0}\frac{p_3}{\varsigma-\varsigma_0} + \psi_0^{I*}(\varsigma)\right] \tag{22c}$$

$$\gamma_{32}^{II} + i\gamma_{31}^{II} = 2u_0^{II*}(\varsigma) \tag{23a}$$

$$E_2^{II} + iE_1^{II} = -2\phi_0^{II*}(\varsigma) \tag{23b}$$

$$H_2^{II} + iH_1^{II} = -2\psi_0^{II*}(\varsigma) \tag{23c}$$

In deriving Eqs. (20)–(23), $\Omega(\varsigma)$ in Eq. (19) has been absorbed to form the new unknown functions, $u_0^*(\varsigma), \phi_0^{I*}(\varsigma), \psi_0^{I*}(\varsigma), u_0^{II*}(\varsigma), \phi_0^{II*}(\varsigma), \psi_0^{II*}(\varsigma)$.

3. Hilbert problems and solutions

In this section, the conditions on the interface and the crack face are used to derive the Hilbert problems, from the solutions of which the magnetoelectroelastic fields can be obtained.

3.1. The interface conditions

Substituting the magnetoelectroelastic fields in Eqs. (20)–(23) into the interface conditions in Eqs. (1)–(3) leads to

$$\begin{aligned}&\frac{\sigma_3}{4\pi i}\frac{\bar z_0}{\bar\varsigma_0}\frac{1}{\xi-\bar\varsigma_0} + C_{44}^I u_0^{I*+}(\xi) + e_{15}^I\phi_0^{I*+}(\xi) + h_{15}^I\psi_0^{I*+}(\xi)\\ &- C_{44}^{II}\overline{u}_0^{II*+}(\xi) - e_{15}^{II}\overline{\phi}_0^{II*+}(\xi) - h_{15}^{II}\overline{\psi}_0^{II*+}(\xi)\\ &= \frac{\sigma_3}{4\pi i}\frac{z_0}{\varsigma_0}\frac{1}{\xi-\varsigma_0} + C_{44}^{II} u_0^{II*-}(\xi) + e_{15}^{II}\phi_0^{II*-}(\xi) + h_{15}^{II}\psi_0^{I*-}(\xi)\\ &- C_{44}^I\overline{u}_0^{I*-}(\xi) - e_{15}^I\overline{\phi}_0^{I*-}(\xi) - h_{15}^I\overline{\psi}_0^{I*-}(\xi)\end{aligned} \tag{24}$$

$$\begin{aligned}&\frac{q_{e0}}{4\pi i}\frac{\bar z_0}{\bar\varsigma_0}\frac{1}{\xi-\bar\varsigma_0} + e_{15}^I u_0^{I*+}(\xi) - \varepsilon_{11}^{I\phi_0^{I*+}}(\xi) - \beta_{11}^I\psi_0^{I*+}(\xi) - e_{15}^{II}\overline{u}_0^{II*+}(\xi)\\ &+ \varepsilon_{11}^{II}\overline{\phi}_0^{II*+}(\xi) + \beta_{11}^{II}\overline{\psi}_0^{II*+}(\xi)\\ &= \frac{q_{e0}}{4\pi i}\frac{z_0}{\varsigma_0}\frac{1}{\xi-\varsigma_0} + e_{15}^{II} u_0^{II*-}(\xi) - \varepsilon_{11}^{II}\phi_0^{II*-}(\xi) - \beta_{11}^{II}\psi_0^{I*-}(\xi)\\ &- e_{15}^I\overline{u}_0^{I*-}(\xi) + \varepsilon_{11}^I\overline{\phi}_0^{I*-}(\xi) + \beta_{11}^I\overline{\psi}_0^{I*-}(\xi)\end{aligned} \tag{25}$$

$$\begin{aligned}&\frac{q_{m0}}{4\pi i}\frac{\bar z_0}{\bar\varsigma_0}\frac{1}{\xi-\bar\varsigma_0} + h_{15}^I u_0^{I*+}(\xi) - \beta_{11}^I\phi_0^{I*+}(\xi) - \mu_{11}^I\psi_0^{I*+}(\xi)\\ &- h_{15}^{II}\overline{u}_0^{II*+}(\xi) + \beta_{11}^{II}\overline{\phi}_0^{II*+}(\xi) + \mu_{11}^{II}\overline{\psi}_0^{II*+}(\xi)\\ &= \frac{q_{m0}}{4\pi i}\frac{z_0}{\varsigma_0}\frac{1}{\xi-\varsigma_0} + h_{15}^{II} u_0^{II*-}(\xi) - \beta_{11}^{II}\phi_0^{II*-}(\xi) - \mu_{11}^{II}\psi_0^{I*-}(\xi)\\ &- h_{15}^I\overline{u}_0^{I*-}(\xi) + \beta_{11}^I\overline{\phi}_0^{I*-}(\xi) + \mu_{11}^I\overline{\psi}_0^{I*-}(\xi)\end{aligned} \tag{26}$$

$$-\frac{\bar z_0}{\bar\varsigma_0}\frac{\bar p_1}{\xi-\bar\varsigma_0} + u_0^{I*+}(\xi) + \overline{u}_0^{II*+}(\xi) = -\frac{z_0}{\varsigma_0}\frac{p_1}{\xi-\varsigma_0} + u_0^{II*-}(\xi) + \overline{u}_0^{I*-}(\xi) \tag{27}$$

$$-\frac{\bar z_0}{\bar\varsigma_0}\frac{\bar p_2}{\xi-\bar\varsigma_0} + \phi_0^{I*+}(\xi) + \overline{\phi}_0^{II*+}(\xi) = -\frac{z_0}{\varsigma_0}\frac{p_2}{\xi-\varsigma_0} + \phi_0^{II*-}(\xi) + \overline{\phi}_0^{I*-}(\xi) \tag{28}$$

$$-\frac{\bar z_0}{\bar\varsigma_0}\frac{\bar p_3}{\xi-\bar\varsigma_0} + \psi_0^{I*+}(\xi) + \overline{\psi}_0^{II*+}(\xi) = -\frac{z_0}{\varsigma_0}\frac{p_3}{\xi-\varsigma_0} + \psi_0^{II*-}(\xi) + \overline{\psi}_0^{I*-}(\xi) \tag{29}$$

where an over bar represent complex conjugate. The analytical continuation technique has been used. For example, an analytical function $\bar\phi(\varsigma)$ can be introduced so that, on the real axis, there exists $\bar\phi^+(\xi) = \overline{\phi^-(\xi)}$ if $\phi(\varsigma)$ is defined and analytical on the lower half-plane, or $\bar\phi^-(\xi) = \overline{\phi^+(\xi)}$ if $\phi(\varsigma)$ is defined and analytical on the upper half-plane. It should be noted that in Eqs. (24)–(29), there is $\xi \in L_1 \cup L_2$. Now introduce six new functions $M(\varsigma), N(\varsigma), P(\varsigma), Q(\varsigma), R(\varsigma), T(\varsigma)$ as follows,

$$M(\varsigma) = \begin{cases} V_1(\varsigma) + C_{44}^I u_0^{I*}(\varsigma) + e_{15}^I\phi_0^{I*}(\varsigma) + h_{15}^I\psi_0^{I*}(\varsigma) - C_{44}^{II}\overline{u_0^{II*}}(\varsigma) - e_{15''}\overline{\phi_0^{II*}}(\varsigma) - h_{15}^{II}\overline{\psi_0^{II*}} & (\varsigma) \quad \eta > 0\\ V_2(\varsigma) + C_{44}^{II} u_0^{II*}(\varsigma) + e_{15}^{II}\phi_0^{II*}(\varsigma) + h_{15}^{II}\psi_0^{I^*(\varsigma)} - C_{44}^I\overline{u_0^{I*}}(\varsigma) - e_{15}^I\overline{\phi_0^{I*}}(\varsigma) - h_{15}^I\overline{\psi_0^{I*}}(\varsigma) & \eta < 0\end{cases} \tag{30a, b}$$

$$N(\varsigma) = \begin{cases} V_3(\varsigma) + e_{15}^I u_0^{I*}(\varsigma) - \varepsilon_{11}^I\phi_0^{I*}(\varsigma) - \beta_{11}^I\psi_0^{I^*}(\varsigma) - e_{15}^{II}\overline{u_0^{II*}}(\varsigma) + \varepsilon_{11}^{II}\overline{\phi_0^{II*}}(\varsigma) + \beta_{11}^{II}\overline{\psi_0^{II*}}(\varsigma) & \eta > 0\\ V_4(\varsigma) + e_{15}^{II} u_0^{II*}(\varsigma) - \varepsilon_{11}^{II}\phi_0^{II*}(\varsigma) - \beta_{11}^{II}\psi_0^{I^*}(\varsigma) - e_{15}^I\overline{u_0^{I*}}(\varsigma) + \varepsilon_{11}^I\overline{\phi_0^{I*}}(\varsigma) + \beta_{11}^I\overline{\psi_0^{I*}}(\varsigma) & \eta < 0\end{cases} \tag{31a, b}$$

$$P(\varsigma) = \begin{cases} V_5(\varsigma) + h_{15}^I u_0^{I*}(\varsigma) - \beta_{11}^I\phi_0^{I*}(\varsigma) - \mu_{11}^I\psi_0^{I*}(\varsigma) - h_{15}^{II}\overline{u_0^{II*}}(\varsigma) + \beta_{11}^{II}\overline{\phi_0^{II*}}(\varsigma) + \mu_{11}^{II}\overline{\psi_0^{II*}}(\varsigma) & \eta > 0\\ V_6(\varsigma) + h_{15}^{II} u_0^{II*}(\varsigma) - \beta_{11}^{II}\phi_0^{II*}(\varsigma) - \mu_{11}^{II}\psi_0^{I^*}(\varsigma) - h_{15}^I\overline{u_0^{I*}}(\varsigma) + \beta_{11}^I\overline{\phi_0^{I*}}(\varsigma) + \mu_{11}^I\overline{\psi_0^{I*}}(\varsigma) & \eta < 0\end{cases} \tag{32a, b}$$

$$Q(\varsigma)=\begin{cases} V_7(\varsigma)+u_0^{I*}(\varsigma)+\overline{u_0^{II*}}(\varsigma) & \eta>0 \\ V_8(\varsigma)+u_0^{II*}(\varsigma)+\overline{u_0^{I*}}(\varsigma) & \eta<0 \end{cases} \tag{33a, b}$$

$$R(\varsigma)=\begin{cases} V_9(\varsigma)+\phi_0^{I*}(\varsigma)+\overline{\phi_0^{II*}}(\varsigma) & \eta>0 \\ V_{10}(\varsigma)+\phi_0^{II*}(\varsigma)+\overline{\phi_0^{I*}}(\varsigma) & \eta<0 \end{cases} \tag{34a, b}$$

$$T(\varsigma)=\begin{cases} V_{11}(\varsigma)+\psi_0^{I*}(\varsigma)+\overline{\psi_0^{II*}}(\varsigma) & \eta>0 \\ V_{12}(\varsigma)+\psi_0^{II*}(\varsigma)+\overline{\psi_0^{I*}}(\varsigma) & \eta<0 \end{cases} \tag{35a, b}$$

where $V_i(\varsigma)(i=1,2,\ldots,12)$ are given in Appendix B. Eqs. (30a)–(35a) and Eqs. (30b)–(35b) can be, respectively, arranged into two sets of simultaneous equations, from which the unknown functions can be solved as follows,

$$u_0^{I*}(\varsigma)=\frac{1}{G}\begin{bmatrix}\lambda_1^a M(\varsigma)+\lambda_2^a N(\varsigma)+\lambda_3^a P(\varsigma)+\lambda_4^a Q(\varsigma)+\lambda_5^a R(\varsigma)+\lambda_6^a T(\varsigma)\\ -\lambda_1^a V_1(\varsigma)-\lambda_2^a V_3(\varsigma)-\lambda_3^a V_5(\varsigma)-\lambda_4^a V_7(\varsigma)-\lambda_5^a V_9(\varsigma)-\lambda_6^a V_{11}(\varsigma)\end{bmatrix} \tag{36}$$

$$\phi_0^{I*}(\varsigma)=\frac{1}{G}\begin{bmatrix}\lambda_1^b M(\varsigma)+\lambda_2^b N(\varsigma)+\lambda_3^b P(\varsigma)+\lambda_4^b Q(\varsigma)+\lambda_5^b R(\varsigma)+\lambda_6^b T(\varsigma)\\ -\lambda_1^b V_1(\varsigma)-\lambda_2^b V_3(\varsigma)-\lambda_3^b V_5(\varsigma)-\lambda_4^b V_7(\varsigma)-\lambda_5^b V_9(\varsigma)-\lambda_6^b V_{11}(\varsigma)\end{bmatrix} \tag{37}$$

$$\psi_0^{I*}(\varsigma)=\frac{1}{G}\begin{bmatrix}\lambda_1^d M(\varsigma)+\lambda_2^d N(\varsigma)+\lambda_3^d P(\varsigma)+\lambda_4^d Q(\varsigma)+\lambda_5^d R(\varsigma)+\lambda_6^d T(\varsigma)\\ -\lambda_1^d V_1(\varsigma)-\lambda_2^d V_3(\varsigma)-\lambda_3^d V_5(\varsigma)-\lambda_4^d V_7(\varsigma)-\lambda_5^d V_9(\varsigma)-\lambda_6^d V_{11}(\varsigma)\end{bmatrix} \tag{38}$$

$$u_0^{II*}(\varsigma)=\frac{1}{G}\begin{bmatrix}\lambda_1^a M(\varsigma)+\lambda_2^a N(\varsigma)+\lambda_3^a P(\varsigma)+\lambda^v Q(\varsigma)-\lambda_5^a R(\varsigma)-\lambda_6^a T(\varsigma)\\ -\lambda_1^a V_2(\varsigma)-\lambda_2^a V_4(\varsigma)-\lambda_3^a V_6(\varsigma)-\lambda^v V_8(\varsigma)+\lambda_5^a V_{10}(\varsigma)+\lambda_6^a V_{12}(\varsigma)\end{bmatrix} \tag{39}$$

$$\phi_0^{II*}(\varsigma)=\frac{1}{G}\begin{bmatrix}\lambda_1^b M(\varsigma)+\lambda_2^b N(\varsigma)+\lambda_3^b P(\varsigma)-\lambda_4^b Q(\varsigma)+\lambda^w R(\varsigma)-\lambda_6^b T(\varsigma)\\ -\lambda_1^b V_2(\varsigma)-\lambda_2^b V_4(\varsigma)-\lambda_3^b V_6(\varsigma)+\lambda_4^b V_8(\varsigma)-\lambda^w V_{10}(\varsigma)+\lambda_6^b V_{12}(\varsigma)\end{bmatrix} \tag{40}$$

$$\psi_0^{I*}(\varsigma)=\frac{1}{G}\begin{bmatrix}\lambda_1^d M(\varsigma)+\lambda_2^d N(\varsigma)+\lambda_3^d P(\varsigma)-\lambda_4^d Q(\varsigma)-\lambda_5^d R(\varsigma)+\lambda^y T(\varsigma)\\ -\lambda_1^d V_2(\varsigma)-\lambda_2^d V_4(\varsigma)-\lambda_3^d V_6(\varsigma)+\lambda_4^d V_8(\varsigma)+\lambda_5^d V_{10}(\varsigma)-\lambda^y V_{12}(\varsigma)\end{bmatrix} \tag{41}$$

$$\overline{u_0^{II*}}(\varsigma)=\frac{1}{G}\begin{bmatrix}-\lambda_1^a M(\varsigma)-\lambda_2^a N(\varsigma)-\lambda_3^a P(\varsigma)+\lambda^v Q(\varsigma)-\lambda_5^a R(\varsigma)-\lambda_6^a T(\varsigma)\\ +\lambda_1^a V_1(\varsigma)+\lambda_2^a V_3(\varsigma)+\lambda_3^a V_5(\varsigma)-\lambda^v V_7(\varsigma)+\lambda_5^a V_9(\varsigma)+\lambda_6^a V_{11}(\varsigma)\end{bmatrix} \tag{42}$$

$$\overline{\phi_0^{II*}}(\varsigma)=\frac{1}{G}\begin{bmatrix}-\lambda_1^b M(\varsigma)-\lambda_2^b N(\varsigma)-\lambda_3^b P(\varsigma)-\lambda_4^b Q(\varsigma)+\lambda^w R(\varsigma)-\lambda_6^b T(\varsigma)\\ +\lambda_1^b V_1(\varsigma)+\lambda_2^b V_3(\varsigma)+\lambda_3^b V_5(\varsigma)+\lambda_4^b V_7(\varsigma)-\lambda^w V_9(\varsigma)+\lambda_6^b V_{11}(\varsigma)\end{bmatrix} \tag{43}$$

$$\overline{\psi_0^{II*}}(\varsigma)=\frac{1}{G}\begin{bmatrix}-\lambda_1^d M(\varsigma)-\lambda_2^d N(\varsigma)-\lambda_3^d P(\varsigma)-\lambda_4^d Q(\varsigma)-\lambda_5^d R(\varsigma)+\lambda^y T(\varsigma)\\ +\lambda_1^d V_1(\varsigma)+\lambda_2^d V_3(\varsigma)+\lambda_3^d V_5(\varsigma)+\lambda_4^d V_7(\varsigma)+\lambda_5^d V_9(\varsigma)-\lambda^y V_{11}(\varsigma)\end{bmatrix} \tag{44}$$

$$\overline{u_0^{I*}}(\varsigma)=\frac{1}{G}\begin{bmatrix}-\lambda_1^a M(\varsigma)-\lambda_2^a N(\varsigma)-\lambda_3^a P(\varsigma)+\lambda_4^a Q(\varsigma)+\lambda_5^a R(\varsigma)+\lambda_6^a T(\varsigma)\\ +\lambda_1^a V_2(\varsigma)+\lambda_2^a V_4(\varsigma)+\lambda_3^a V_6(\varsigma)-\lambda_4^a V_8(\varsigma)-\lambda_5^a V_{10}(\varsigma)-\lambda_6^a V_{12}(\varsigma)\end{bmatrix} \tag{45}$$

$$\overline{\phi_0^{I*}}(\varsigma)=\frac{1}{G}\begin{bmatrix}-\lambda_1^b M(\varsigma)-\lambda_2^b N(\varsigma)-\lambda_3^b P(\varsigma)+\lambda_4^b Q(\varsigma)+\lambda_5^b R(\varsigma)+\lambda_6^b T(\varsigma)\\ +\lambda_1^b V_2(\varsigma)+\lambda_2^b V_4(\varsigma)+\lambda_3^b V_6(\varsigma)-\lambda_4^b V_8(\varsigma)-\lambda_5^b V_{10}(\varsigma)-\lambda_6^b V_{12}(\varsigma)\end{bmatrix} \tag{46}$$

$$\overline{\psi_0^{I*}}(\varsigma)=\frac{1}{G}\begin{bmatrix}-\lambda_1^d M(\varsigma)-\lambda_2^d N(\varsigma)-\lambda_3^d P(\varsigma)+\lambda_4^d Q(\varsigma)+\lambda_5^d R(\varsigma)+\lambda_6^d T(\varsigma)\\ +\lambda_1^d V_2(\varsigma)+\lambda_2^d V_4(\varsigma)+\lambda_3^d V_6(\varsigma)-\lambda_4^d V_8(\varsigma)-\lambda_5^d V_{10}(\varsigma)-\lambda_6^d V_{12}(\varsigma)\end{bmatrix} \tag{47}$$

where the coefficients $\lambda_i^a(i=1\ldots6)$, $\lambda_i^b(i=1\ldots6)$, $\lambda_i^d(i=1\ldots6)$, λ^v, λ^w and λ^y are listed in Appendix C. The parameter G is defined as

$$G=\left(e_{15}^I+e_{15}^{II}\right)^2\left(\mu_{11}^I+\mu_{11}^{II}\right)+\left(h_{15}^I+h_{15}^{II}\right)^2\left(\varepsilon_{11}^I+\varepsilon_{11}^{II}\right)-\left(\beta_{11}^I+\beta_{11}^{II}\right)^2\left(C_{44}^I+C_{44}^{II}\right)-2\left(e_{15}^I+e_{15}^{II}\right)\left(h_{15}^I+h_{15}^{II}\right)\left(\beta_{11}^I+\beta_{11}^{II}\right)+\left(C_{44}^I+C_{44}^{II}\right)\left(\varepsilon_{11}^I+\varepsilon_{11}^{II}\right)\left(\mu_{11}^I+\mu_{11}^{II}\right) \tag{48}$$

3.2. Conditions on the crack faces

The conditions on the crack faces in the mapping plane can be provided in terms of Eqs. (4)–(6), as follows,

$$\tau_{31}^I(\xi,0^+)=\tau_{31}^{II}(\xi,0^-)=0 \tag{49a, b}$$

$$D_1^I(\xi,0^+)=D_1^{II}(\xi,0^-)=0 \tag{50a, b}$$

$$B_1^I(\xi,0^+)=B_1^{II}(\xi,0^-)=0 \tag{51a, b}$$

where ξ is confined to $\xi\in L$. Substituting the magnetoelectroelastic fields in Eqs. (20) and (21) into Eqs. (49)–(51) leads to the following identities,

$$-\frac{\sigma_3}{4\pi i}\frac{\bar z_0}{\bar\varsigma_0}\frac{1}{\xi-\bar\varsigma_0}+C_{44}^I u_0^{I+}(\xi)+e_{15}^I\phi_0^{I+}(\xi)+h_{15}^I\psi_0^{I+}(\xi)=\frac{\sigma_3}{4\pi i}\frac{z_0}{\varsigma_0}\frac{1}{\xi-\varsigma_0}+C_{44}^I\overline{u_0^{I-}}(\xi)+e_{15}^I\overline{\phi_0^{I-}}(\xi)+h_{15}^I\overline{\psi_0^{I-}}(\xi) \tag{52a}$$

$$C_{44}^{II}\overline{u_0^{II+}}(\xi)+e_{15}^{II}\overline{\phi_0^{II+}}(\xi)+h_{15}^{II}\overline{\psi_0^{II+}}(\xi)=C_{44}^{II}u_0^{II-}(\xi)+e_{15}^{II}\phi_0^{II-}(\xi)+h_{15}^{II}\psi_0^{II-}(\xi) \tag{52b}$$

$$-\frac{q_{e0}}{4\pi i}\frac{\bar z_0}{\bar\varsigma_0}\frac{1}{\xi-\bar\varsigma_0}+e_{15}^I u_0^{I+}(\xi)-\varepsilon_{11}^I\phi_0^{I+}(\xi)-\beta_{11}^I\psi_0^{I+}(\xi)=\frac{q_{e0}}{4\pi i}\frac{z_0}{\varsigma_0}\frac{1}{\xi-\varsigma_0}+e_{15}^I\overline{u_0^{I-}}(\xi)-\varepsilon_{11}^I\overline{\phi_0^{I-}}(\xi)-\beta_{11}^I\overline{\psi_0^{I-}}(\xi) \tag{53a}$$

$$-e_{15}^{II}\overline{u_0^{II+}}(\xi)+\varepsilon_{11}^{II}\overline{\phi_0^{II+}}(\xi)+\beta_{11}^{II}\overline{\psi_0^{II+}}(\xi)=-e_{15}^{II}u_0^{II-}(\xi)+\varepsilon_{11}^{II}\phi_0^{II-}(\xi)+\beta_{11}^{II}\psi_0^{II-}(\xi) \tag{53b}$$

$$-\frac{q_{m0}}{4\pi i}\frac{\bar z_0}{\bar\varsigma_0}\frac{1}{\xi-\bar\varsigma_0}+h_{15}^I u_0^{I+}(\xi)-\beta_{11}^I\phi_0^{I+}(\xi)-\mu_{11}^I\psi_0^{I+}(\xi)=\frac{q_{m0}}{4\pi i}\frac{z_0}{\varsigma_0}\frac{1}{\xi-\varsigma_0}+h_{15}^I\overline{u_0^{I-}}(\xi)-\beta_{11}^I\overline{\phi_0^{I-}}(\xi)-\mu_{11}^I\overline{\psi_0^{I-}}(\xi) \tag{54a}$$

$$-h_{15}^{II}\overline{u_0^{II+}}(\xi)+\beta_{11}^{II}\overline{\phi_0^{II+}}(\xi)+\mu_{11}^{II}\overline{\psi_0^{II+}}(\xi)=-h_{15}^{II}u_0^{II-}(\xi)+\beta_{11}^{II}\phi_0^{II-}(\xi)+\mu_{11}^{II}\psi_0^{II-}(\xi) \tag{54b}$$

By using Eqs. (52)–(54), and taking notice of Eqs. (32)–(34), after tedious manipulation and arrangements of equations, the following Hilbert problems can be formulated.

$$\begin{cases} M^+(\xi)-M^-(\xi)=0 & \xi\in L_1\cup L_2 \\ M^+(\xi)+M^-(\xi)=\frac{\sigma_3}{2\pi i}\frac{\bar z_0}{\bar\varsigma_0}\frac{1}{\xi-\bar\varsigma_0}+\frac{\sigma_3}{2\pi i}\frac{z_0}{\varsigma_0}\frac{1}{\xi-\varsigma_0} & \xi\in L \end{cases} \tag{55a, b}$$

$$\begin{cases} N^+(\xi)-N^-(\xi)=\xi\in L_1\cup L_2 \\ N^+(\xi)+N^-(\xi)=\frac{q_{e0}}{2\pi i}\frac{\bar z_0}{\bar\varsigma_0}\frac{1}{\xi-\bar\varsigma_0}+\frac{q_{e0}}{2\pi i}\frac{z_0}{\varsigma_0}\frac{1}{\xi-\varsigma_0} & \xi\in L \end{cases} \tag{56a, b}$$

$$\begin{cases} P^+(\xi)-P^-(\xi)=0 & \xi\in L_1\cup L_2 \\ P^+(\xi)+P^-(\xi)=\frac{q_{m0}}{2\pi i}\frac{\bar z_0}{\bar\varsigma_0}\frac{1}{\xi-\bar\varsigma_0}+\frac{q_{m0}}{2\pi i}\frac{z_0}{\varsigma_0}\frac{1}{\xi-\varsigma_0} & \xi\in L \end{cases} \tag{57a, b}$$

$$Q^+(\xi)-Q^-(\xi)=0 \quad \xi\in L_1\cup L\cup L_2 \tag{58}$$

$$R^+(\xi)-R^-(\xi)=0 \quad \xi\in L_1\cup L\cup L_2 \tag{59}$$

$$T^+(\xi)-T^-(\xi)=0 \quad \xi\in L_1\cup L\cup L_2 \tag{60}$$

3.3. Solutions to the Hilbert problems

The fundamental solution to the Hilbert problems in Eqs. (55)–(57) is Xiao and Xie (2008)

$$X(\varsigma)=(\varsigma+a)^{-\frac{1}{2}}(\varsigma-a)^{-\frac{1}{2}}\varsigma^{-1} \tag{61}$$

In terms of the complex variable method (Muskhelishvili,1975), the complete solutions to Eqs. (55)–(57) can be obtained as follows,

$$M(\varsigma)=-V_1(\varsigma)-V_2(\varsigma)+X(\varsigma)\left[\frac{\sigma_3}{4\pi i}\left(\frac{\bar{z}_0^2}{\varsigma-\bar{\varsigma}_0}+\frac{z_0^2}{\varsigma-\varsigma_0}\right)+c_{M1}\varsigma+c_{M0}\right] \tag{62}$$

$$N(\varsigma)=-V_3(\varsigma)-V_4(\varsigma)+X(\varsigma)\left[\frac{q_{e0}}{4\pi i}\left(\frac{\bar{z}_0^2}{\varsigma-\bar{\varsigma}_0}+\frac{z_0^2}{\varsigma-\varsigma_0}\right)+c_{N1}\varsigma+c_{N0}\right] \tag{63}$$

$$P(\varsigma)=-V_5(\varsigma)-V_6(\varsigma)+X(\varsigma)\left[\frac{q_{m0}}{4\pi i}\left(\frac{\bar{z}_0^2}{\varsigma-\bar{\varsigma}_0}+\frac{z_0^2}{\varsigma-\varsigma_0}\right)+c_{P1}\varsigma+c_{P0}\right] \tag{64}$$

where $c_{M1}, c_{M0}, c_{N1}, c_{N0}, c_{P1}, c_{P0}$ are constants to be determined. One should bear in mind that the magnetoelectroelastic fields at B' and D', which do not correspond to the crack tips in the z plane, must be nonsingular. In Eqs. (62)–(64), no item except $X(\varsigma)$ is singular at B' and D'. It can be concluded that the formula in the square brackets in Eqs. (62)–(64) must vanish when $\varsigma \to a+0$ or $\varsigma \to -a-0$. Based on these requirements, the constants can be determined as follows,

$$c_{M1}=\frac{\sigma_3}{2\pi i}, \quad c_{M0}=\frac{Re(\varsigma_0)\sigma_3}{2\pi i} \tag{65a, b}$$

$$c_{N1}=\frac{q_{e0}}{2\pi i}, \quad c_{N0}=\frac{Re(\varsigma_0)q_{e0}}{2\pi i} \tag{66a, b}$$

$$c_{P1}=\frac{q_{m0}}{2\pi i}, \quad c_{P0}=\frac{Re(\varsigma_0)q_{m0}}{2\pi i} \tag{67a, b}$$

where $Re[\bullet]$ represents the real part. Eqs. (62)–(64) can then be rearranged in a concise form as follows,

$$M(\varsigma)=-[V_1(\varsigma)+V_2(\varsigma)]+\sigma_3 S_1(\varsigma) \tag{68}$$

$$N(\varsigma)=-[V_3(\varsigma)+V_4(\varsigma)]+q_{e0} S_1(\varsigma) \tag{69}$$

$$P(\varsigma)=-[V_5(\varsigma)+V_6(\varsigma)]+q_{m0} S_1(\varsigma) \tag{70}$$

where

$$S_1(\varsigma)=\frac{X(\varsigma)}{4\pi i}\left[\frac{\overline{z_0}^2}{\varsigma-\bar{\varsigma}_0}+\frac{z_0^2}{\varsigma-\varsigma_0}+2\varsigma+2Re(\varsigma_0)\right] \tag{71}$$

To find the solutions for $Q(\varsigma), R(\varsigma)$ and $T(\varsigma)$, we should be aware that the magnetoelectroelastic fields are singular at $\varsigma=0$, which corresponds to the crack tips in the physical plane (Xiao and Xie, 2008). In terms of the generalized Liouville theorem (Muskhelishivili,1975), from Eqs. (58)–(60), we find,

$$Q(\varsigma)=V_7(\varsigma)+V_8(\varsigma)+\frac{c_Q}{\varsigma} \tag{72}$$

$$R(\varsigma)=V_9(\varsigma)+V_{10}(\varsigma)+\frac{c_R}{\varsigma} \tag{73}$$

$$T(\varsigma)=V_{11}(\varsigma)+V_{12}(\varsigma)+\frac{c_T}{\varsigma} \tag{74}$$

where c_Q, c_R and c_T are constants which should be determined by the single-valued condition of the displacement, electric potential and magnetic potential. For example, to determine c_Q, the following equation can be used,

$$\oint_\Gamma Q(\varsigma)\omega'(\varsigma)d\varsigma=0 \tag{75}$$

where Γ is the contour around L in ς plane. The other two constants can similarly be determined. Finally, c_Q, c_R and c_T can be found,

$$c_Q=2ip_1 Im\left(\frac{z_0}{\varsigma_0}\right), \quad c_R=2ip_2 Im\left(\frac{z_0}{\varsigma_0}\right),$$
$$c_T=2ip_3 Im\left(\frac{z_0}{\varsigma_0}\right) \tag{76a, b, c}$$

3.4. The analytical solution to the magnetoelectroelastic fields

Once the functions $M(\varsigma), N(\varsigma), P(\varsigma), Q(\varsigma), R(\varsigma), T(\varsigma)$ are obtained, the magnetoelectroelastic fields on the entire plane can be analytically found

$$\tau_{32}^I+i\tau_{31}^I=\frac{2}{G}\left\{(\sigma_3K_1^\tau+q_{e0}K_2^\tau+q_{m0}K_3^\tau)[S_1(\varsigma)-S_2(\varsigma)]-\frac{1}{2\pi\varsigma}\left(\lambda_4^a\sigma_3+\lambda_4^bq_{e0}+\lambda_4^dq_{m0}\right)Im\left(\frac{z_0}{\varsigma_0}\right)\right\} \tag{77}$$

$$\tau_{32}^{II}+i\tau_{31}^{II}=\frac{2}{G}\left\{-\left[\sigma_3\left(K_1^\tau-G\right)+q_{e0}K_2^\tau+q_{m0}K_3^\tau\right][S_1(\varsigma)-S_2(\varsigma)]-\frac{1}{2\pi\varsigma}\left(\lambda_4^a\sigma_3+\lambda_4^bq_{e0}+\lambda_4^dq_{m0}\right)Im\left(\frac{z_0}{\varsigma_0}\right)\right\} \tag{78}$$

$$D_2^I+iD_1^I=\frac{2}{G}\left\{\left(\sigma_3K_1^D+q_{e0}K_2^D+q_{m0}K_3^D\right)[S_1(\varsigma)-S_2(\varsigma)]-\frac{1}{2\pi\varsigma}\left(\lambda_5^a\sigma_3+\lambda_5^bq_{e0}+\lambda_5^dq_{m0}\right)Im\left(\frac{z_0}{\varsigma_0}\right)\right\} \tag{79}$$

$$D_2^{II}+iD_1^{II}=\frac{2}{G}\left\{-\left[\sigma_3K_1^D-q_{e0}\left(G-K_2^D\right)+q_{m0}K_3^D\right][S_1(\varsigma)-S_2(\varsigma)]-\frac{1}{2\pi\varsigma}\left(\lambda_5^a\sigma_3+\lambda_5^bq_{e0}+\lambda_5^dq_{m0}\right)Im\left(\frac{z_0}{\varsigma_0}\right)\right\} \tag{80}$$

$$B_2^I+iB_1^I=\frac{2}{G}\left\{\left(\sigma_3K_1^B+q_{e0}K_2^B+q_{m0}K_3^B\right)[S_1(\varsigma)-S_2(\varsigma)]-\frac{1}{2\pi\varsigma}\left(\lambda_6^a\sigma_3+\lambda_6^bq_{e0}+\lambda_6^dq_{m0}\right)Im\left(\frac{z_0}{\varsigma_0}\right)\right\} \tag{81}$$

$$B_2^{II}+iB_1^{II}=\frac{2}{G}\left\{-\left[\sigma_3K_1^B+q_{e0}K_2^B-q_{m0}\left(G-K_3^B\right)\right][S_1(\varsigma)-S_2(\varsigma)]-\frac{1}{2\pi\varsigma}\left(\lambda_6^a\sigma_3+\lambda_6^bq_{e0}+\lambda_6^dq_{m0}\right)Im\left(\frac{z_0}{\varsigma_0}\right)\right\} \tag{82}$$

$$\gamma_{32}^I+i\gamma_{31}^I=\frac{2}{G}\left\{(\sigma_3\lambda_1^a+q_{e0}\lambda_2^a+q_{m0}\lambda_3^a)[S_1(\varsigma)-S_2(\varsigma)]-\frac{1}{2\pi\varsigma}(\sigma_3K_1^\gamma+q_{e0}K_2^\gamma+q_{m0}K_3^\gamma)Im\left(\frac{z_0}{\varsigma_0}\right)\right\} \tag{83}$$

$$\gamma_{32}^{II}+i\gamma_{31}^{II}=\frac{2}{G}\left\{(\sigma_3\lambda_1^a+q_{e0}\lambda_2^a+q_{m0}\lambda_3^a)[S_1(\varsigma)-S_2(\varsigma)]-\frac{1}{2\pi\varsigma}(\sigma_3\lambda_1^a+q_{e0}\lambda_2^a+q_{m0}\lambda_3^a)Im\left(\frac{z_0}{\varsigma_0}\right)\right\} \tag{84}$$

$$E_2^I+iE_1^I=-\frac{2}{G}\left\{\left(\sigma_3\lambda_1^b+q_{e0}\lambda_2^b+q_{m0}\lambda_3^b\right)[S_1(\varsigma)-S_2(\varsigma)]-\frac{1}{2\pi\varsigma}\left(\sigma_3K_1^E+q_{e0}K_2^E+q_{m0}K_3^E\right)Im\left(\frac{z_0}{\varsigma_0}\right)\right\} \tag{85}$$

$$E_2^{II}+iE_1^{II}=-\frac{2}{G}\left\{\left(\sigma_3\lambda_1^b+q_{e0}\lambda_2^b+q_{m0}\lambda_3^b\right)[S_1(\varsigma)-S_2(\varsigma)]-\frac{1}{2\pi\varsigma}\left(\sigma_3\lambda_1^b+q_{e0}\lambda_2^b+q_{m0}\lambda_3^b\right)Im\left(\frac{z_0}{\varsigma_0}\right)\right\} \tag{86}$$

$$H_2^I+iH_1^I=-\frac{2}{G}\left\{\left(\sigma_3\lambda_1^d+q_{e0}\lambda_2^d+q_{m0}\lambda_3^d\right)[S_1(\varsigma)-S_2(\varsigma)]-\frac{1}{2\pi\varsigma}\left(\sigma_3K_1^H+q_{e0}K_2^H+q_{m0}K_3^H\right)Im\left(\frac{z_0}{\varsigma_0}\right)\right\} \tag{87}$$

$$H_2^{II}+iH_1^{II}=-\frac{2}{G}\left\{\left(\sigma_3\lambda_1^d+q_{e0}\lambda_2^d+q_{m0}\lambda_3^d\right)[S_1(\varsigma)-S_2(\varsigma)]-\frac{1}{2\pi\varsigma}\left(\sigma_3\lambda_1^d+q_{e0}\lambda_2^d+q_{m0}\lambda_3^d\right)Im\left(\frac{z_0}{\varsigma_0}\right)\right\} \tag{88}$$

where

$$S_2(\varsigma)=\frac{1}{2\pi i}\left(\frac{z_0}{\varsigma_0}\frac{1}{\varsigma-\varsigma_0}+\frac{\bar{z}_0}{\bar{\varsigma}_0}\frac{1}{\varsigma-\bar{\varsigma}_0}\right) \tag{89}$$

The coefficients $K_i^{\tau}(i=1\ldots3)$, $K_i^{D}(i=1\ldots3)$, $K_i^{B}(i=1\ldots3)$, $K_i^{\gamma}(i=1\ldots3)$, $K_i^{E}(i=1\ldots3)$, $K_i^{H}(i=1\ldots3)$ are listed in Appendix D.

3.5. The intensity factors for the magnetoelectroelastic fields around the crack tips

By substituting respectively $z=ia+re^{i\theta}$ and $z=-ia+re^{i\theta}$ into Eqs. (77)–(88), and letting $r\to0$ as well as neglecting the high order infinitesimal items, the magnetoelectroelastic fields around the crack tips can be obtained, as listed in Appendix E. The intensity factors for the crack tip A in the upper half-plane can be obtained by letting $\theta=\pi/2$ in Eqs. (E.1), (E.3), (E.5), (E.7), (E.9) and (E.11). These intensity factors render as follows,

$$k_{\tau_{31}^{I}}=\frac{1}{G}\sqrt{\frac{1}{\pi a}}\left[(\sigma_3K_1^{\tau}+q_{e0}K_2^{\tau}+q_{m0}K_3^{\tau})aRe\left(\frac{1}{\varsigma_0}\right)+\left(\lambda_4^{a}\sigma_3+\lambda_4^{b}q_{e0}+\lambda_4^{d}q_{m0}\right)Im\left(\frac{z_0}{\varsigma_0}\right)\right] \tag{90}$$

$$k_{D_1^{I}}=\frac{1}{G}\sqrt{\frac{1}{\pi a}}\left[\left(\sigma_3K_1^{D}+q_{e0}K_2^{D}+q_{m0}K_3^{D}\right)aRe\left(\frac{1}{\varsigma_0}\right)+\left(\lambda_5^{a}\sigma_3+\lambda_5^{b}q_{e0}+\lambda_5^{d}q_{m0}\right)Im\left(\frac{z_0}{\varsigma_0}\right)\right] \tag{91}$$

$$k_{B_1^{I}}=\frac{1}{G}\sqrt{\frac{1}{\pi a}}\left[\left(\sigma_3K_1^{B}+q_{e0}K_2^{B}+q_{m0}K_3^{B}\right)aRe\left(\frac{1}{\varsigma_0}\right)+\left(\lambda_6^{a}\sigma_3+\lambda_6^{b}q_{e0}+\lambda_6^{d}q_{m0}\right)Im\left(\frac{z_0}{\varsigma_0}\right)\right] \tag{92}$$

$$k_{\gamma_{31}^{I}}=\frac{1}{G}\sqrt{\frac{1}{\pi a}}\left[(\sigma_3\lambda_1^{a}+q_{e0}\lambda_2^{a}+q_{m0}\lambda_3^{a})aRe\left(\frac{1}{\varsigma_0}\right)+(\sigma_3K_1^{\gamma}+q_{e0}K_2^{\gamma}+q_{m0}K_3^{\gamma})Im\left(\frac{z_0}{\varsigma_0}\right)\right] \tag{93}$$

$$k_{E_1^{I}}=-\frac{1}{G}\sqrt{\frac{1}{\pi a}}\left[\left(\sigma_3\lambda_1^{b}+q_{e0}\lambda_2^{b}+q_{m0}\lambda_3^{b}\right)aRe\left(\frac{1}{\varsigma_0}\right)+\left(\sigma_3K_1^{E}+q_{e0}K_2^{E}+q_{m0}K_3^{E}\right)Im\left(\frac{z_0}{\varsigma_0}\right)\right] \tag{94}$$

$$k_{H_1^{I}}=-\frac{1}{G}\sqrt{\frac{1}{\pi a}}\left[\left(\sigma_3\lambda_1^{d}+q_{e0}\lambda_2^{d}+q_{m0}\lambda_3^{d}\right)aRe\left(\frac{1}{\varsigma_0}\right)+\left(\sigma_3K_1^{H}+q_{e0}K_2^{H}+q_{m0}K_3^{H}\right)Im\left(\frac{z_0}{\varsigma_0}\right)\right] \tag{95}$$

Similarly, by letting $\theta=3\pi/2$ in Eqs. (E.2), (E.4), (E.6), (E.8), (E.10) and (E.12), the intensity factors for the crack tip C in the lower half-plane can be obtained,

$$k_{\tau_{31}^{II}}=\frac{1}{G}\sqrt{\frac{1}{\pi a}}\left\{-\left[\sigma_3\left(K_1^{\tau}-G\right)+q_{e0}K_2^{\tau}+q_{m0}K_3^{\tau}\right]aRe\left(\frac{1}{\varsigma_0}\right)-\left(\lambda_4^{a}\sigma_3+\lambda_4^{b}q_{e0}+\lambda_4^{d}q_{m0}\right)Im\left(\frac{z_0}{\varsigma_0}\right)\right\} \tag{96}$$

$$k_{D_1^{II}}=\frac{1}{G}\sqrt{\frac{1}{\pi a}}\left\{-\left[\sigma_3K_1^{D}-q_{e0}\left(G-K_2^{D}\right)+q_{m0}K_3^{D}\right]aRe\left(\frac{1}{\varsigma_0}\right)-\left(\lambda_5^{a}\sigma_3+\lambda_5^{b}q_{e0}+\lambda_5^{d}q_{m0}\right)Im\left(\frac{z_0}{\varsigma_0}\right)\right\} \tag{97}$$

$$k_{B_1^{II}}=\frac{1}{G}\sqrt{\frac{1}{\pi a}}\left\{-\left[\sigma_3K_1^{B}+q_{e0}K_2^{B}-q_{m0}\left(G-K_3^{B}\right)\right]aRe\left(\frac{1}{\varsigma_0}\right)-\left(\lambda_6^{a}\sigma_3+\lambda_6^{b}q_{e0}+\lambda_6^{d}q_{m0}\right)Im\left(\frac{z_0}{\varsigma_0}\right)\right\} \tag{98}$$

$$k_{\gamma_{31}^{II}}=\frac{1}{G}\sqrt{\frac{1}{\pi a}}\left[(\sigma_3\lambda_1^{a}+q_{e0}\lambda_2^{a}+q_{m0}\lambda_3^{a})aRe\left(\frac{1}{\varsigma_0}\right)-(\sigma_3\lambda_1^{a}+q_{e0}\lambda_2^{a}+q_{m0}\lambda_3^{a})Im\left(\frac{z_0}{\varsigma_0}\right)\right] \tag{99}$$

$$k_{E_1^{II}}=-\frac{1}{G}\sqrt{\frac{1}{\pi a}}\left[\left(\sigma_3\lambda_1^{b}+q_{e0}\lambda_2^{b}+q_{m0}\lambda_3^{b}\right)aRe\left(\frac{1}{\varsigma_0}\right)-\left(\sigma_3\lambda_1^{b}+q_{e0}\lambda_2^{b}+q_{m0}\lambda_3^{b}\right)Im\left(\frac{z_0}{\varsigma_0}\right)\right] \tag{100}$$

$$k_{H_1^{II}}=-\frac{1}{G}\sqrt{\frac{1}{\pi a}}\left[\left(\sigma_3\lambda_1^{d}+q_{e0}\lambda_2^{d}+q_{m0}\lambda_3^{d}\right)aRe\left(\frac{1}{\varsigma_0}\right)-\left(\sigma_3\lambda_1^{d}+q_{e0}\lambda_2^{d}+q_{m0}\lambda_3^{d}\right)Im\left(\frac{z_0}{\varsigma_0}\right)\right] \tag{101}$$

3.6. Discussions on the intensity factors

In this subsection, we discuss the intensity factors for some special cases. We first verify that the solution to the semi-infinite elastic bimaterial with a mode III crack cutting perpendicularly across the interface can be recovered. If we choose the vanishing piezoelectric, piezomagnetic and magnetoelectric coefficients, i.e., $e_{15}^1=e_{15}^2=0$, $h_{15}^1=h_{15}^2=0$ and $\beta_{11}^1=\beta_{11}^2=0$, and also letting $q_{e0}=q_{m0}=0$, the SIFs given by Eqs. (90) and (96) reduce to those in Xiao and Xie (2008).

Next, we consider the mode III crack in an infinite homogeneous magnetoelectroelastic, piezoelectric or piezomagnetic material subjected respectively to a concentrated magnetoelectroelastic, electromechanical or magnetomechanical load at an arbitrary position in the upper half-plane. These problems can be included as the special cases by the solution of this paper. Suppose the upper and lower half planes have the same magnetoelectroelastic media, then an infinite homogeneous magnetoelectroelastic material with a through mode III crack is recovered. The intensity factors can be obtained,

$$k_{\tau_{31}^{I}}=\frac{\sigma_3}{2\sqrt{\pi a}}R_1(a,z_0),\quad k_{D_1^{I}}=\frac{q_{e0}}{2\sqrt{\pi a}}R_1(a,z_0),\quad k_{B_1^{I}}=\frac{q_{m0}}{2\sqrt{\pi a}}R_1(a,z_0) \tag{102a,b,c}$$

$$k_{\tau_{31}^{II}}=\frac{\sigma_3}{2\sqrt{\pi a}}R_2(a,z_0),\quad k_{D_1^{II}}=\frac{q_{e0}}{2\sqrt{\pi a}}R_2(a,z_0),\quad k_{B_1^{II}}=\frac{q_{m0}}{2\sqrt{\pi a}}R_2(a,z_0) \tag{103a,b,c}$$

where

$$R_1(a,z_0)=aRe\left(\frac{1}{\varsigma_0}\right)+Im\left(\frac{z_0}{\varsigma_0}\right),\quad R_2(a,z_0)=aRe\left(\frac{1}{\varsigma_0}\right)-Im\left(\frac{z_0}{\varsigma_0}\right) \tag{104a,b,c}$$

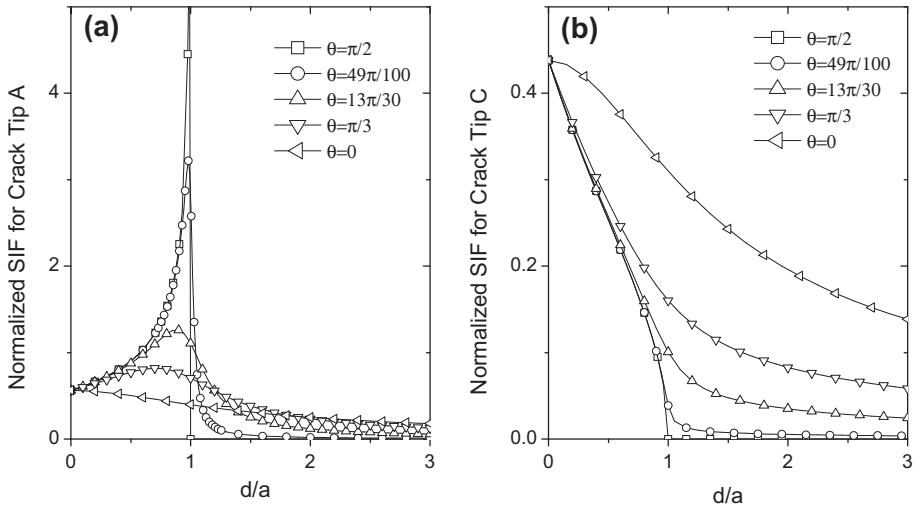

Fig. 2. The normalized SIF versus position distance, d/a, under a line force for (a) Crack tip A, $k'_{\tau_{31}^I}$ (b) Crack tip C, $k'_{\tau_{31}^{II}}$.

It can be seen from Eqs. (102) and (103) that the SIFs, the EDIFs and the MIIFs depend only upon the line force, the line electric charge and the line magnetic charge, respectively. The SIFs for both crack tips vanish if no line force is applied. The EDIFs vanish for both crack tips if the line electric charge is removed. These conclusions agree to the general statement for the mode III crack in an infinite homogeneous piezoelectric with impermeable conditions on crack face in Zhang et al. (2002). Furthermore, if the line force is only confined on the crack face, then the SIFs can be obtained, in terms of the solution of this paper,

$$k_{\tau_{31}^I} = \frac{\sigma_3}{2\sqrt{a\pi}}\sqrt{\frac{a+y}{a-y}}, \quad k_{\tau_{31}^{II}} = \frac{\sigma_3}{2\sqrt{a\pi}}\sqrt{\frac{a-y}{a+y}} \tag{105a, b}$$

Eqs. (105a,b) are identical to previous results in literature, such as in Gao and Wang (2001).

For the general cases of dissimilar magnetoelectroelastic semi-infinite bimaterials, the intensity factors usually depend on all kinds of the loads, except the case that the load is applied on the crack extension line where all the magnetoelectroelastic fields vanish. For examples, if only a line force is considered, the EDIFs and MIIFs are generally not vanishing. Moreover, the EDIFs as well as the MIIFs are identical for both crack tips in magnitude but opposite in sign, irrespective of the load position, as shown in Eqs. (106a,b). Similarly, if only a line electric charge is applied, the SIFs as well as the MIIFs generally do not vanish, and are equal for both crack tips in magnitude but opposite in sign, disregarding the location of the line electric charge. Actually, Eq. (106a,b)–(108a,b) are all identities when only a line force, a line electric charge and a line magnetic charge is considered, respectively, no matter where the location is. This is quite different from the mode III crack in an infinite homogeneous media.

$$k_{D_1^I} = -k_{D_1^{II}}, \quad k_{B_1^I} = -k_{B_1^{II}} \tag{106a, b}$$

$$k_{\tau_{31}^I} = -k_{\tau_{31}^{II}}, \quad k_{B_1^I} = -k_{B_1^{II}} \tag{107a, b}$$

$$k_{\tau_{31}^I} = -k_{\tau_{31}^{II}}, \quad k_{D_1^I} = -k_{D_1^{II}} \tag{108a, b}$$

The physical interpretation can be given as follows. The electric displacement and magnetic induction obey the conservation law if no electric charge or magnetic charge exists in the magnetoelectroelastic solid. For the impermeable conditions on crack face, no electrical line or magnetical line can pass through and intersect with the crack faces. The electrical lines or magnetical lines that flow into one tip of the crack must flow out from the other tip. The concentration of electric displacement or magnetic induction must be exactly the same for the two crack tips, irrespective of the location of the applied line force. Therefore, the EDIFs, as well as the MIIFs, are

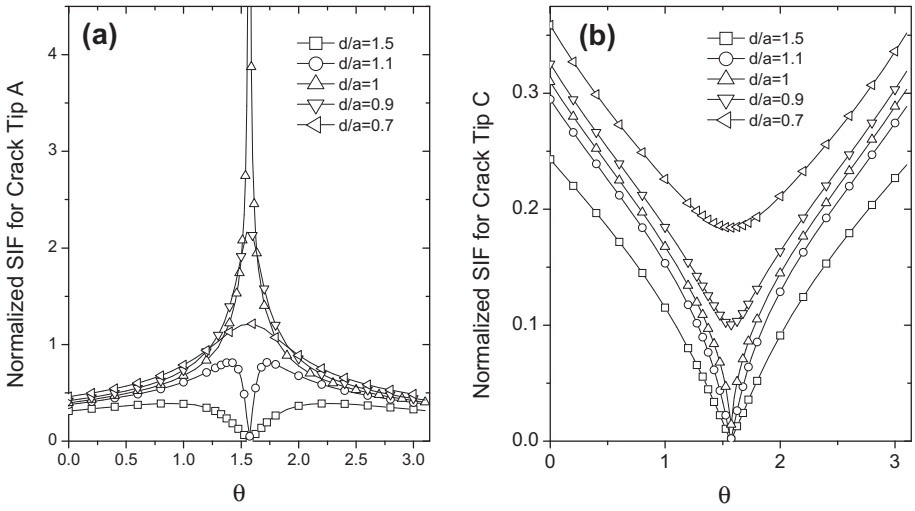

Fig. 3. The normalized SIF versus position angle, θ, under a line force, (a) Crack tip A, $k'_{\tau_{31}^I}$ (b) Crack tip C, $k'_{\tau_{31}^{II}}$.

identical for both tips in magnitude but opposite in sign. In terms of the reciprocal theorem, the electric charge or magnetic charge induced stress should also exhibit the same behavior as the stress-induced electric displacement or magnetic induction. The generated mechanical stress must have the same behavior in the vicinity of the crack tips. They should have the same intensity factor but opposite in direction, no matter where the load location is.

4. Example analysis and discussions

In this section, by using concrete material costants, some numerical calculations will be carried out. The intensity factors are graphically demonstrated. Discussions are presented with respect to the load position and the material constants.

4.1. The intensity factors versus the load position

In this subsection, we graphically present the intensity factors versus the load position, i.e., the distance and the position angle, (d,θ), for both crack tips which lie respectively in the upper and lower magnetoelectroelastic plane. To focus on the discussion of load position, we just consider a line force, i.e., $q_{e0}=q_{m0}=0$. To do the numerical calculation, material constants should be specified. Without loss of generality, we choose the magnetoelectroelastic constants as follows, (Zhong and Li, 2006)

$$\begin{aligned} &C^I_{44}=4.4\times10^{10}\ \mathrm{N/m^2},\quad e^I_{15}=5.8\ \mathrm{C/m^2},\\ &h^I_{15}=275\ \mathrm{N/Am},\quad \varepsilon^I_{11}=5.64\times10^{-9}\ \mathrm{C^2/Nm^2},\\ &\mu^I_{11}=-2.97\times10^{-4}\ \mathrm{Ns^2/C^2},\quad \beta^I_{11}=5.367\times10^{-12}\ \mathrm{Ns/VC}, \end{aligned} \tag{109}$$

for the upper half-plane, and

$$\begin{aligned} &C^{II}_{44}=3.4\times10^{10}\ \mathrm{N/m^2},\quad e^{II}_{15}=4.8\ \mathrm{C/m^2},\\ &h^{II}_{15}=195\ \mathrm{N/Am},\quad \varepsilon^{II}_{11}=4.64\times10^{-9}\mathrm{C^2/Nm^2},\\ &\mu^{II}_{11}=-2.01\times10^{-4}\ \mathrm{Ns^2/C^2},\quad \beta^{II}_{11}=4\times10^{-12}\ \mathrm{Ns/VC}, \end{aligned} \tag{110}$$

for the lower half-plane. The SIFs have been analytically given in Eq. (90) for crack tip A, and Eq. (96) for crack tip C. It is convenient to adopt dimensionless parameters in the plots so that we define the normalized SIFs as follows,

$$k_{\tau^I_{31}}=\frac{\sigma_3}{\sqrt{a\pi}}k'_{\tau^I_{31}},\quad k_{\tau^{II}_{31}}=\frac{\sigma_3}{\sqrt{a\pi}}k'_{\tau^{II}_{31}} \tag{111}$$

where $k'_{\tau^I_{31}}$ and $k'_{\tau^{II}_{31}}$ are the normalized SIF for the crack tip A and C, respectively. Since the EDIFs are identical in magnitude for both two

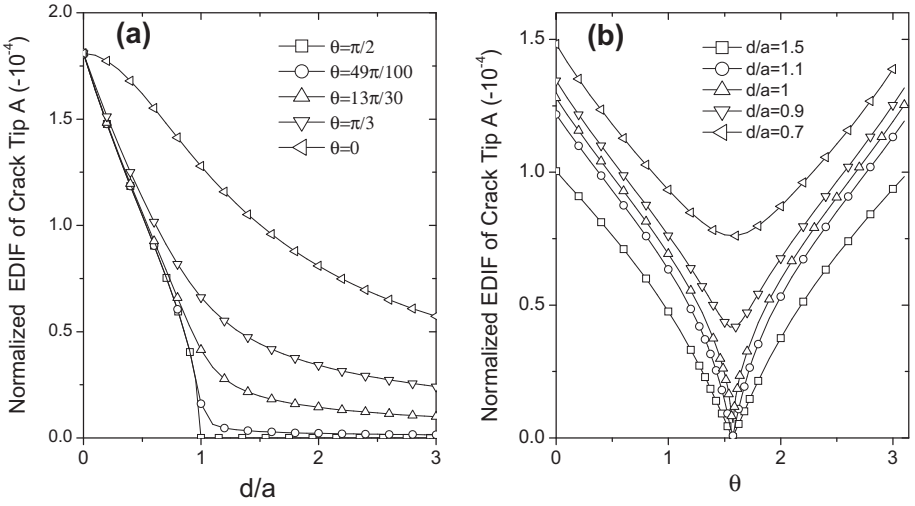

Fig. 4. The normalized EDIF for crack tip A, $k'_{D^I_1}$, under a line force versus (a) position distance d/a (b) position angle, θ.

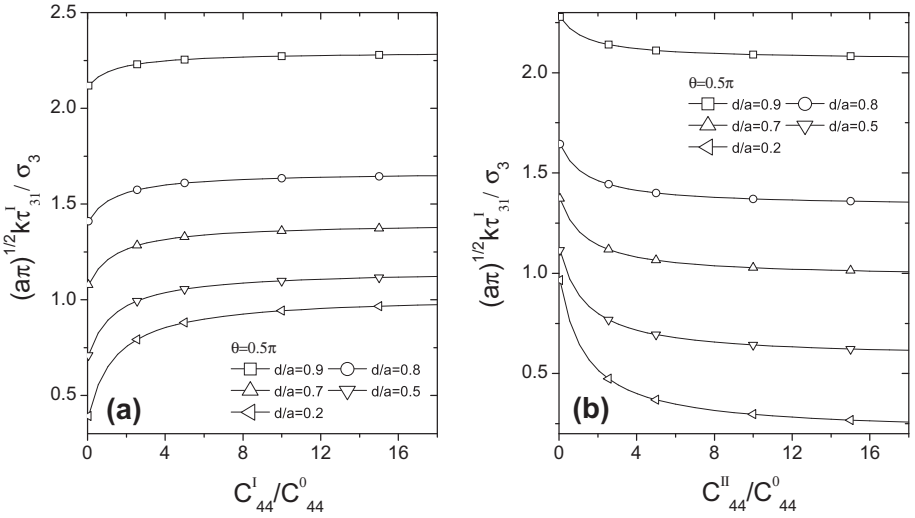

Fig. 5. The normalized SIF for crack tip A versus (a) C^I_{44}/C^0_{44} and (b) C^{II}_{44}/C^0_{44} under a line force.

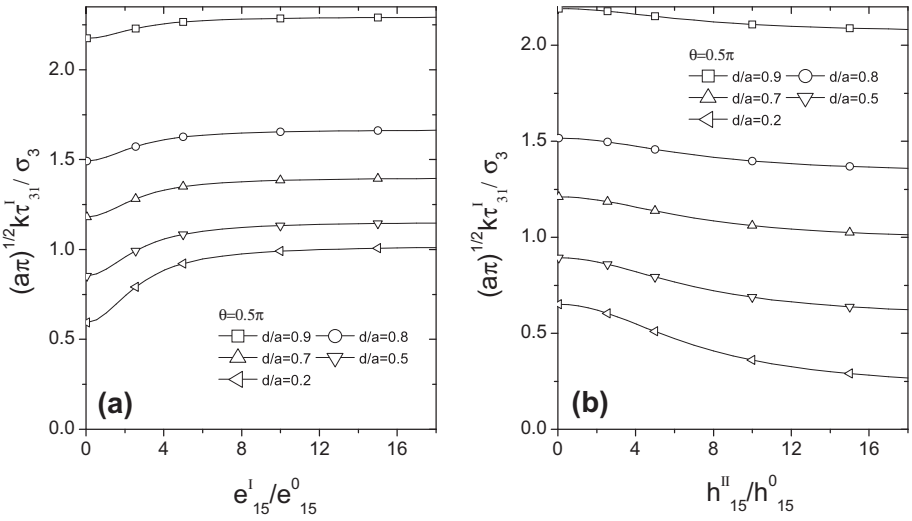

Fig. 6. The normalized SIF for crack tip A versus (a) e^{I}_{15}/e^{0}_{15} and (b) h^{II}_{15}/h^{0}_{15} under a line force.

crack tips, only one of them needs to be studied. The following normalized EDIF for crack tip A will be used in the plots.

$$k_{D^I_1} = \frac{\sigma_3}{\sqrt{\pi a}} \frac{\varepsilon^I_{11}}{e^I_{15}} k'_{D^I_1} \tag{112}$$

in which $k'_{D^I_1}$ is the normalized EDIF for the crack tip A. Fig. 2 shows the normalized SIFs plotted against the normalized distance (d/a) under a line force. In Fig. 2(a), the normalized SIF of crack tip A defined in Eq. (111a) is plotted against distance for different position angles. The general situation can be found that the SIF decreases as the force moves away from the crack tip A, or vice versa. Let us consider the case of $\theta = \pi/2$, where the line force is confined on the crack face or the crack extension line on the upper half-plane. When the load is exactly located at the crack center, i.e., $d = 0$, the SIFs are identical for both crack tips. As d increases, indicating the force is getting near the crack tip A and away from the crack tip C, the SIF of crack tip A increases and tends to be infinite when $d = a$. Oppositely, the SIF of crack tip C decreases and finally reduces to zero. As noted previously, the SIFs vanish for both crack tips when the load is on the crack extension line. There is an abrupt jump for the SIF of crack tip A when the line force moves from the crack face to the crack extension line, as shown in Fig. 2(a). The same behavior for the SIF can also be found in Xiao and Xie (2008). Fig. 2(b) shows the variation of the normalized SIF for crack tip C, given in Eq. (111b), along with the position distance, while the position angle is kept as different constants. It can be seen in Fig. 2(b), the normalized SIF for crack tip C generally decreases as d increases. For a larger θ within the scope $(0, \pi/2)$, the SIF descends more steeply. It is in agreement to the common sense that the SIF for a crack tip decreases as the line force moves away from the tip itself. Fig. 3 presents the normalized SIFs for both crack tips versus the position angle θ. The plots are symmetrical with respect to $\theta = \pi/2$. For a certain distance, the SIF become invariant when the load is, respectively, located symmetrically with respect to the x_2 axis in the first quadrant and second quadrant of the z plane. Also the fact can be confirmed by the plots that a shorter distance leads to a larger SIF, or vice versa.

The normalized EDIF for crack tip A, as given in Eq. (112), is plotted against the distance (d/a) in Fig. 4(a) as well as position angle (θ) in Fig. 4(b). It can be seen in Fig. 4(b), when the distance is kept as a constant, the EDIF is symmetrical with respect to $\theta = \pi/2$. Hence, the dependence of the EDIF on position angle can be discussed just within the scope of $0 \sim \pi/2$. As θ increases from 0 to $\pi/2$, the EDIF monotonically decreases. For a certain θ, as indicated

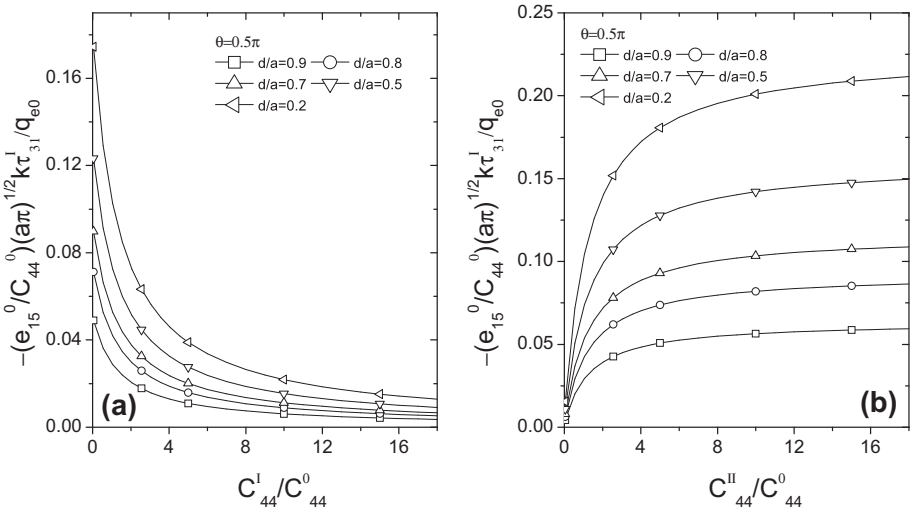

Fig. 7. The normalized SIF for crack tip A versus (a) C^{I}_{44}/C^{0}_{44} and (b) C^{II}_{44}/C^{0}_{44} under a line charge.

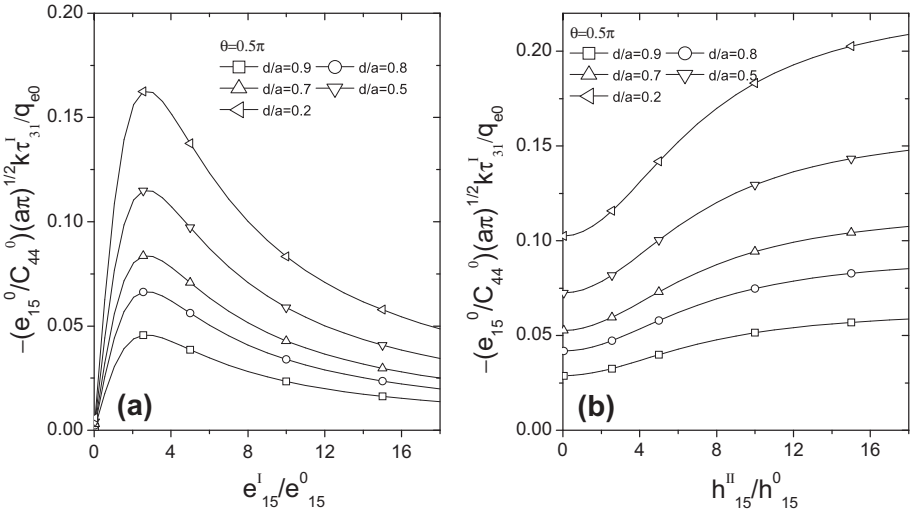

Fig. 8. The normalized SIF for crack tip A versus (a) e^I_{15}/e^0_{15} and (b) h^{II}_{15}/h^0_{15} under a line charge.

in Fig. 4(a), the EDIF generally decreases as the distance d increases. For example, when $\theta = \pi/2$, the EDIF descends most steeply to zero as the distance d increase from 0 to a. Therefore, as the line force is approaching the crack tip A, the EDIF decreases to zero, which is complete opposite to the SIF as discussed previously. Furthermore, it can also be found that, the EDIF attains the maximum when $d = 0$, i.e., the line force is acting at the crack center. The EDIF vanishes when the load is applied on the crack extension line, including the crack tips.

Since the MIIF has the similar behavior to the EDIF when only a line force is applied, the discussion of the MIIF is omitted here.

4.2. Variation of the SIF with the material constants

In this subsection, the influence of material constants on the intensity factors will be explored. Since the SIF is generally the most concern factor for a crack problem, we just focus on the normalized SIF for the upper crack tip, i.e., crack tip A. To facilitate the discussion, the general magnetoelectroelastic bimaterial is reduced to the piezoelectric/piezomagnetic bimaterial, where the upper half-plane is piezoelectric (e.g. $BaTiO_3$), and the lower half-plane is piezomagnetic (e.g. $CoFe_2O_4$). The following constants can be found (Wang et al., 2010),

$$C^I_{44} = 4.3\times10^{10}\ \mathrm{N/m^2},\quad e^I_{15} = 11.6\ C/\mathrm{m^2},\quad \varepsilon^I_{11} = 11.2\times10^{-9}\ \mathbf{C}^2/\mathrm{Nm^2},\quad \mu^I_{11} = 5\times10^{-6}\ \mathrm{Ns^2}/C^2 \tag{113a}$$

$$C^{II}_{44} = 4.53\times10^{10}\ \mathrm{N/m^2},\quad h^{II}_{15} = 550\ \mathrm{N/Am},\quad \varepsilon^{II}_{11} = 0.08\times10^{-9}\ C^2/\mathrm{Nm^2},\quad \mu^{II}_{11} = 157\times10^{-6}\ \mathrm{Ns^2}/C^2 \tag{113b}$$

Other constants vanish, i.e.,

$$h^I_{15} = 0,\quad \beta^I_{11} = 0,\quad e^{II}_{15} = 0,\quad \beta^{II}_{11} = 0 \tag{113c}$$

The separately applied line force or line charge will be considered. The dependence of the normalized SIF for crack tip A on the shear moduli and the piezo constitutive coefficients will be graphically shown, where the following constants are used in the normalization.

$$C^0_{44} = 4.3\times10^{10}\mathrm{N/m^2},\quad e^0_{15} = 11.6C/\mathrm{m^2},$$
$$h^0_{15} = 550\mathrm{N/Am} \tag{114a, b, c}$$

To explore the influences of the shear moduli, the material constants in Eqs. (110a,b,c) will be used except the shear moduli C^I_{44} and C^{II}_{44}, which are recognized as variables. Shown in Fig. 5(a) and (b) are the normalized SIF plotted against the normalized shear modulus of the piezoelectric, C^I_{44}/C^0_{44}, and the piezomagnetic, C^{II}_{44}/C^0_{44}, respectively. It can be seen the normalized SIF monotonically increases and decreases with respect to C^I_{44} and C^{II}_{44}, respectively. The interpretation can be given by considering the respective share of the applied line force by the upper and lower materials. According to the simple mix rule for the overall modulus of a composite, if the modulus of the upper part increases, the load shared by the upper part enhances, which results in a larger SIF around crack tip A. Conversely, if the lower part become more rigid, then the SIF for tip A decreases, as shown in Fig. 5(a) and (b). Fig. 6(a) and (b) give the variation of the normalized SIF with the normalized piezo constitutive constants. The material constants in Eqs. (113a,b,c) are used except the piezoelectric coefficient e^I_{15} and piezomagnetic coefficient h^{II}_{15}, which are considered as variables. The SIF increases or decreases as e^I_{15} or h^{II}_{15} increases, respectively. The underlying physics is related with the piezo stiffening effect, which can be expressed as,

$$\frac{c^E}{c^D} = 1 - k_e^2,\quad \frac{c^H}{c^B} = 1 - k_m^2 \tag{115a, b}$$

where c^E, c^H are the short-circuit elastic moduli, c^D, c^B the open-circuit elastic moduli, $k_e k_m$ the electromechanical and magnetomechanical coupling coefficient defined as $k_e = e^I_{15}/\sqrt{c^I_{44}\varepsilon^I_{11}}, k_m = h^{II}_{15}/\sqrt{c^{II}_{44}\mu^{II}_{11}}$. As the piezo constitutive coefficients increase, the piezo stiffening effect become more pronounced, which result in a larger apparent shear moduli in the upper or lower part. Therefore, in terms of Fig. 5(a) and (b), the SIF increases or decreases as e^I_{15} or h^{II}_{15} increases, respectively.

Given in Figs. 7 and 8 are the results when a line charge is solely applied on the upper half. Under electric loading, the piezoelectric material deforms positively. The piezomagnetic material in the lower half deforms negatively due to the perfect interface, on which tractions are continuous. The application of a line electric charge in the piezoelectric half can be viewed as a strain load that is applied on the two-phase composite of the upper piezoelectric and the lower

piezomagnetic. If one phase becomes more rigid, then this phase shall take a less proportion of the strain load, since both of them should develop the continuous tractions on the interface. Therefore, if the piezoelectric phase becomes more rigid, the SIF decreases since the upper part take a less share of the load, as shown in Fig. 7(a). On the contrary, if the piezomagnetic phase in the lower part becomes more rigid, then the upper part will take a bigger proportion of the load, which enhances the SIF for crack tip A, as indicated in Fig. 7(b).

Fig. 8(a) and (b) illustrate the normalized SIF versus the normalized piezo constitutive coefficients, i.e., e_15^I/e_15^0 and h_15^II/h_15^0. As previously noted, the role of piezo coefficients should be connected with the piezo stiffening effect. For example, an increment of the piezomagnetic coefficient, indicating an enhancement to the apparent modulus of the piezomagnetic phase in the lower half, will invariably increase the SIF for crack tip A. This is shown in Fig. 8(b), where the SIF monotonically increases as h_15^II/h_15^0 increases. Nevertheless, if the piezoelectric coefficient is varied for the case of a line electric charge, two aspects should be involved. One aspect is related to the piezo stiffening effect, which obviously leads to a larger apparent modulus in piezoelectric phase for a bigger e_15^I/e_15^0. Therefore, the load shared by the upper phase decreases. The other aspect lies on the corresponding strain load, which actually diminishes if the peizoelctric coefficient, e, increases. This can be understood as follows: the electric flux density, indicated by D, is composed of two parts, i.e., $D = e\gamma + \varepsilon E$. Since the dielectric permittivity ε is constant, the electric field can be assumed unvaried for the given electric charge. Therefore, an increment of e implies a decrement of the corresponding strain load, γ, since the total electric flux is associated with the given electric charge and should remain unchanged. Hence, whether the proportion of the strain load undertaken by the piezoelectric phase decreases or not depends on the balance of these two aspects. As a matter of fact, as indicated in Fig. 8(a) where the SIF changes non-monotonically as the piezoelectric coefficient increases, there exists a critical value $e_15^I/e_15^0\big|_c$ of the piezoelectric coefficient, before which and after which the SIF increases and decreases monotonically. This critical value can be analytically obtained as,

$$\left.\frac{e_{15}^I}{e_{15}^0}\right|_c = \sqrt{\frac{\left(h_{15}^{II}\right)^2\left(\varepsilon_{11}^I+\varepsilon_{11}^{II}\right)}{\left(e_{15}^0\right)^2\left(\mu_{11}^I+\mu_{11}^{II}\right)}+\frac{\left(\varepsilon_{11}^I+\varepsilon_{11}^{II}\right)\left(C_{44}^I+C_{44}^{II}\right)}{\left(e_{15}^0\right)^2}} \tag{116}$$

5. Conclusions

In this paper, we have analytically obtained the solution of the magnetoelectroelastic fields for dissimilar semi-infinite magnetoelectroelastic bimaterial, where a mode III crack is cutting perpendicularly across the interface. A general concentrated magnetoelectromechanical load is located at an arbitrary position on the upper half-plane, i.e., the combined loads of a line force vertical to the plane, a line electric charge and a line magnetic charge. By using the complex variable method, the analytical solution is obtained for the entire plane. The intensity factors around both crack tips are found for elastic, electric and magnetic fields. It shows that, no matter where the location of the load is, the EDIFs as well as the MIIFs for both crack tips are identical in magnitude but opposite in sign if only a line force is considered. Likewise, if only a line electric charge is applied, then the SIFs and the MIIFs are identical in magnitude for both crack tips but opposite in direction. And if the line magnetic charge is solely considered, then EDIFs and MIIFs exhibit the mentioned behavior. The intensity factors are graphically demonstrated and discussed with respect to the load position. It is found that the SIF for a crack tip tends to be infinite if the applied line force gets near the tip itself, but the EDIF, with the complete opposite trend, tends to be vanishing. Finally, focusing on the piezoelectric and piezomagnetic bimaterial, variation of the SIF along with the moduli as well as the piezo constitutive coefficients is explored. These analyses may provide some guidance for material selection by minimizing the SIF. Of course, it should be pointed out that the SIF alone actually plays a limited role in the fracture analysis of magnetoelectroelastic solids, since the SIF has been shown not suitable for use as fracture criterion for piezoelectric as well as magnetoelectroelastic solids (Fang et al., 2004). Further works on fracture criterion are still needed in the fracture analysis of magnetoelectroelastic solids. In addition, the results obtained in this paper can also serve as the Green's function for the dissimilar magnetoelectroelastic semi-infinite bimaterial with a crack cutting the interface under general magnetoelectromechanical loads.

Acknowledgments

This work was supported by National Natural Science Foundation of China (Project No. 11072179, 11090334) and Shanghai Leading Academic Discipline Project (Project No. B302).

Appendix A

$$\tau_{32}^I + i\tau_{31}^I = 2\left[-\frac{\sigma_3}{4\pi i}\frac{1}{z-z_0} + C_{44}^I u_0^I(z) + e_{15}^I\phi_0^I(z) + h_{15}^I\psi_0^I(z)\right] \tag{A.1}$$

$$D_2^I + iD_1^I = 2\left[-\frac{q_{e0}}{4\pi i}\frac{1}{z-z_0} + e_{15}^I u_0^I(z) - \varepsilon_{11}^I\phi_0^I(z) - \beta_{11}^I\psi_0^I(z)\right] \tag{A.2}$$

$$B_2^I + iB_1^I = 2\left[-\frac{q_{m0}}{4\pi i}\frac{1}{z-z_0} + h_{15}^I u_0^I(z) - \beta_{11}^I\phi_0^I(z) - \mu_{11}^I\psi_0^I(z)\right] \tag{A.3}$$

$$\tau_{32}^{II} + i\tau_{31}^{II} = 2\left[C_{44}^{II}u_0^{II}(z) + e_{15}^{II}\phi_0^{II}(z) + h_{15}^{II}\psi_0^{II}(z)\right] \tag{A.4}$$

$$D_2^{II} + iD_1^{II} = 2\left[e_{15}^{II}u_0^{II}(z) - \varepsilon_{11}^{II}\phi_0^{II}(z) - \beta_{11}^{II}\psi_0^{II}(z)\right] \tag{A.5}$$

$$B_2^{II} + iB_1^{II} = 2\left[h_{15}^{II}u_0^{II}(z) - \beta_{11}^{II}\phi_0^{II}(z) - \mu_{11}^{II}\psi_0^{II}(z)\right] \tag{A.6}$$

$$\gamma_{32}^I + i\gamma_{31}^I = 2\left[\frac{p_1}{z-z_0} + u_0^I(z)\right] \tag{A.7}$$

$$E_2^I + iE_1^I = -2\left[\frac{p_2}{z-z_0} + \phi_0^I(z)\right] \tag{A.8}$$

$$H_2^I + iH_1^I = -2\left[\frac{p_3}{z-z_0} + \psi_0^I(z)\right] \tag{A.9}$$

$$\gamma_{32}^{II} + i\gamma_{31}^{II} = 2u_0^{II}(z) \tag{A.10}$$

$$E_2^{II} + iE_1^{II} = -2\phi_0^{II}(z) \tag{A.11}$$

$$H_2^{II} + iH_1^{II} = -2\psi_0^{II}(z) \tag{A.12}$$

Appendix B

$$V_1(\varsigma) = \frac{\sigma_3}{4\pi i}\frac{\bar{z}_0}{\bar{\varsigma}_0}\frac{1}{\varsigma-\bar{\varsigma}_0} \tag{B.1}$$

$$V_2(\varsigma) = \frac{\sigma_3}{4\pi i}\frac{z_0}{\varsigma_0}\frac{1}{\varsigma-\varsigma_0} \tag{B.2}$$

$$V_3(\varsigma) = \frac{q_{e0}}{4\pi i}\frac{\bar{z}_0}{\bar{\varsigma}_0}\frac{1}{\varsigma-\bar{\varsigma}_0} \tag{B.3}$$

$$V_4(\varsigma) = \frac{q_{e0}}{4\pi i}\frac{z_0}{\varsigma_0}\frac{1}{\varsigma-\varsigma_0} \tag{B.4}$$

$$V_5(\varsigma) = \frac{q_{m0}}{4\pi i}\frac{\bar{z}_0}{\bar{\varsigma}_0}\frac{1}{\varsigma-\bar{\varsigma}_0} \tag{B.5}$$

$$V_6(\varsigma) = \frac{q_{m0}}{4\pi i}\frac{z_0}{\varsigma_0}\frac{1}{\varsigma-\varsigma_0} \tag{B.6}$$

$$V_7(\varsigma) = -\frac{\bar{z}_0}{\bar{\varsigma}_0}\frac{\bar{p}_1}{\varsigma - \bar{\varsigma}_0} \tag{B.7}$$

$$V_8(\varsigma) = -\frac{z_0}{\varsigma_0}\frac{p_1}{\varsigma - \varsigma_0} \tag{B.8}$$

$$V_9(\varsigma) = -\frac{\bar{z}_0}{\bar{\varsigma}_0}\frac{\bar{p}_2}{\varsigma - \bar{\varsigma}_0} \tag{B.9}$$

$$V_{10}(\varsigma) = -\frac{z_0}{\varsigma_0}\frac{p_2}{\varsigma - \varsigma_0} \tag{B.10}$$

$$V_{11}(\varsigma) = -\frac{\bar{z}_0}{\bar{\varsigma}_0}\frac{\bar{p}_3}{\varsigma - \bar{\varsigma}_0} \tag{B.11}$$

$$V_{12}(\varsigma) = -\frac{z_0}{\varsigma_0}\frac{p_3}{\varsigma - \varsigma_0} \tag{B.12}$$

Appendix C

$$\lambda_1^a = \left(\varepsilon_{11}^I + \varepsilon_{11}^{II}\right)\left(\mu_{11}^I + \mu_{11}^{II}\right) - \left(\beta_{11}^I + \beta_{11}^{II}\right)^2 \tag{C.1}$$

$$\lambda_2^a = \left(e_{15}^I + e_{15}^{II}\right)\left(\mu_{11}^I + \mu_{11}^{II}\right) - \left(h_{15}^I + h_{15}^{II}\right)\left(\beta_{11}^I + \beta_{11}^{II}\right) \tag{C.2}$$

$$\lambda_3^a = \left(h_{15}^I + h_{15}^{II}\right)\left(\varepsilon_{11}^I + \varepsilon_{11}^{II}\right) - \left(e_{15}^I + e_{15}^{II}\right)\left(\beta_{11}^I + \beta_{11}^{II}\right) \tag{C.3}$$

$$\lambda_4^a = h_{15}^{II}\lambda_3^a + e_{15}^{II}\lambda_2^a + C_{44}^{II}\lambda_1^a \tag{C.4}$$

$$\lambda_5^a = \left(h_{15}^I + h_{15}^{II}\right)\left(\varepsilon_{11}^{II}\beta_{11}^I - \varepsilon_{11}^I\beta_{11}^{II}\right) + \left(\mu_{11}^I + \mu_{11}^{II}\right)\left(e_{15}^{II}\varepsilon_{11}^I - e_{15}^I\varepsilon_{11}^{II}\right) + \left(\beta_{11}^I + \beta_{11}^{II}\right)\left(e_{15}^I\beta_{11}^{II} - e_{15}^{II}\beta_{11}^I\right) \tag{C.5}$$

$$\lambda_6^a = \left(e_{15}^I + e_{15}^{II}\right)\left(\mu_{11}^{II}\beta_{11}^I - \mu_{11}^I\beta_{11}^{II}\right) + \left(\varepsilon_{11}^I + \varepsilon_{11}^{II}\right)\left(h_{15}^{II}\mu_{11}^I - h_{15}^I\mu_{11}^{II}\right) + \left(\beta_{11}^I + \beta_{11}^{II}\right)\left(h_{15}^I\beta_{11}^{II} - h_{15}^{II}\beta_{11}^I\right) \tag{C.6}$$

$$\lambda_1^b = \left(e_{15}^I + e_{15}^{II}\right)\left(\mu_{11}^I + \mu_{11}^{II}\right) - \left(h_{15}^I + h_{15}^{II}\right)\left(\beta_{11}^I + \beta_{11}^{II}\right) = \lambda_2^a \tag{C.7}$$

$$\lambda_2^b = -\left(h_{15}^I + h_{15}^{II}\right)^2 - \left(C_{44}^I + C_{44}^{II}\right)\left(\mu_{11}^I + \mu_{11}^{II}\right) \tag{C.8}$$

$$\lambda_3^b = \left(e_{15}^I + e_{15}^{II}\right)\left(h_{15}^I + h_{15}^{II}\right) + \left(C_{44}^I + C_{44}^{II}\right)\left(\beta_{11}^I + \beta_{11}^{II}\right) \tag{C.9}$$

$$\lambda_4^b = \left(h_{15}^I + h_{15}^{II}\right)\left(e_{15}^I h_{15}^{II} - e_{15}^{II}h_{15}^I\right) + \left(\mu_{11}^I + \mu_{11}^{II}\right)\left(e_{15}^I C_{44}^{II} - e_{15}^{II}C_{44}^I\right) + \left(\beta_{11}^I + \beta_{11}^{II}\right)\left(C_{44}^I h_{15}^{II} - C_{44}^{II}h_{15}^I\right) \tag{C.10}$$

$$\lambda_5^b = e_{15}^{II}\lambda_1^b - \varepsilon_{11}^{II}\lambda_2^b - \beta_{11}^{II}\lambda_3^b \tag{C.11}$$

$$\lambda_6^b = \left(e_{15}^I + e_{15}^{II}\right)\left(h_{15}^{II}\mu_{11}^I - h_{15}^I\mu_{11}^{II}\right) + \left(h_{15}^I + h_{15}^{II}\right)\left(h_{15}^I\beta_{11}^{II} - h_{15}^{II}\beta_{11}^I\right) + \left(C_{44}^I + C_{44}^{II}\right)\left(\mu_{11}^I\beta_{11}^{II} - \mu_{11}^{II}\beta_{11}^I\right) \tag{C.12}$$

$$\lambda_1^d = \left(h_{15}^I + h_{15}^{II}\right)\left(\varepsilon_{11}^I + \varepsilon_{11}^{II}\right) - \left(e_{15}^I + e_{15}^{II}\right)\left(\beta_{11}^I + \beta_{11}^{II}\right) = \lambda_3^a \tag{C.13}$$

$$\lambda_2^d = \left(e_{15}^I + e_{15}^{II}\right)\left(h_{15}^I + h_{15}^{II}\right) + \left(C_{44}^I + C_{44}^{II}\right)\left(\beta_{11}^I + \beta_{11}^{II}\right) \tag{C.14}$$

$$\lambda_3^d = -\left(e_{15}^I + e_{15}^{II}\right)^2 - \left(C_{44}^I + C_{44}^{II}\right)\left(\varepsilon_{11}^I + \varepsilon_{11}^{II}\right) \tag{C.15}$$

$$\lambda_4^d = \left(e_{15}^I + e_{15}^{II}\right)\left(e_{15}^{II}h_{15}^I - e_{15}^I h_{15}^{II}\right) + \left(\varepsilon_{11}^I + \varepsilon_{11}^{II}\right)\left(C_{44}^{II}h_{15}^I - C_{44}^I h_{15}^{II}\right) + \left(\beta_{11}^I + \beta_{11}^{II}\right)\left(C_{44}^I e_{15}^{II} - C_{44}^{II}e_{15}^I\right) \tag{C.16}$$

$$\lambda_5^d = \left(h_{15}^I + h_{15}^{II}\right)\left(e_{15}^{II}\varepsilon_{11}^I - e_{15}^I\varepsilon_{11}^{II}\right) + \left(C_{44}^I + C_{44}^{II}\right)\left(\varepsilon_{11}^I\beta_{11}^{II} - \varepsilon_{11}^{II}\beta_{11}^I\right) \tag{C.17}$$

$$\lambda_6^d = h_{15}^{II}\lambda_1^d - \mu_{11}^{II}\lambda_3^d - \beta_{11}^{II}\lambda_2^d \tag{C.18}$$

$$\lambda^v = h_{15}^I\lambda_3^a + e_{15}^I\lambda_2^a + C_{44}^I\lambda_1^a \tag{C.19}$$

$$\lambda^w = e_{15}^I\lambda_1^b - \varepsilon_{11}^I\lambda_2^b - \beta_{11}^I\lambda_3^b \tag{C.20}$$

$$\lambda^y = h_{15}^I\lambda_1^d - \beta_{11}^I\lambda_2^d - \mu_{11}^I\lambda_3^d \tag{C.21}$$

Appendix D

$$K_1^\tau = C_{44}^I\lambda_1^a + e_{15}^I\lambda_1^b + h_{15}^I\lambda_1^d \tag{D.1}$$

$$K_2^\tau = C_{44}^I\lambda_2^a + e_{15}^I\lambda_2^b + h_{15}^I\lambda_2^d = -\left(C_{44}^{II}\lambda_2^a + e_{15}^{II}\lambda_2^b + h_{15}^{II}\lambda_2^d\right) \tag{D.2}$$

$$K_3^\tau = C_{44}^I\lambda_3^a + e_{15}^I\lambda_3^b + h_{15}^I\lambda_3^d = -\left(C_{44}^{II}\lambda_3^a + e_{15}^{II}\lambda_3^b + h_{15}^{II}\lambda_3^d\right) \tag{D.3}$$

$$K_1^D = \left(e_{15}^I\lambda_1^a - \varepsilon_{11}^I\lambda_1^b - \beta_{11}^I\lambda_1^d\right) = -\left(e_{15}^{II}\lambda_1^a - \varepsilon_{11}^{II}\lambda_1^b - \beta_{11}^{II}\lambda_1^d\right) \tag{D.4}$$

$$K_2^D = e_{15}^I\lambda_2^a - \varepsilon_{11}^I\lambda_2^b - \beta_{11}^I\lambda_2^d \tag{D.5}$$

$$K_3^D = e_{15}^I\lambda_3^a - \varepsilon_{11}^I\lambda_3^b - \beta_{11}^I\lambda_3^d = -\left(e_{15}^{II}\lambda_3^a - \varepsilon_{11}^{II}\lambda_3^b - \beta_{11}^{II}\lambda_3^d\right) \tag{D.6}$$

$$K_1^B = h_{15}^I\lambda_1^a - \beta_{11}^I\lambda_1^b - \mu_{11}^I\lambda_1^d = -\left(h_{15}^{II}\lambda_1^a - \beta_{11}^{II}\lambda_1^b - \mu_{11}^{II}\lambda_1^d\right) \tag{D.7}$$

$$K_2^B = h_{15}^I\lambda_2^a - \beta_{11}^I\lambda_2^b - \mu_{11}^I\lambda_2^d = -\left(h_{15}^{II}\lambda_2^a - \beta_{11}^{II}\lambda_2^b - \mu_{11}^{II}\lambda_2^d\right) \tag{D.8}$$

$$K_3^B = h_{15}^I\lambda_3^a - \beta_{11}^I\lambda_3^b - \mu_{11}^I\lambda_3^d \tag{D.9}$$

$$K_1^\gamma = -\lambda_1^a + \frac{\left(\varepsilon_{11}^I\mu_{11}^I - \left(\beta_{11}^I\right)^2\right)G}{\rho} \tag{D.10}$$

$$K_2^\gamma = -\lambda_2^a + \frac{\left(e_{15}^I\mu_{11}^I - h_{15}^I\beta_{11}^I\right)G}{\rho} \tag{D.11}$$

$$K_3^\gamma = -\lambda_3^a + \frac{\left(h_{15}^I\varepsilon_{11}^I - e_{15}^I\beta_{11}^I\right)G}{\rho} \tag{D.12}$$

$$K_1^E = -\lambda_1^b + \frac{\left(e_{15}^I\mu_{11}^I - h_{15}^I\beta_{11}^I\right)G}{\rho} \tag{D.13}$$

$$K_2^E = -\lambda_2^b - \frac{\left(\left(h_{15}^I\right)^2 + C_{44}^I\mu_{11}^I\right)G}{\rho} \tag{D.14}$$

$$K_3^E = -\lambda_3^b + \frac{\left(e_{15}^I h_{15}^I + C_{44}^I\beta_{11}^I\right)G}{\rho} \tag{D.15}$$

$$K_1^H = -\lambda_1^d + \frac{\left(h_{15}^I\varepsilon_{11}^I - e_{15}^I\beta_{11}^I\right)G}{\rho} \tag{D.16}$$

$$K_2^H = -\lambda_2^d + \frac{\left(e_{15}^I h_{15}^I + C_{44}^I\beta_{11}^I\right)G}{\rho} \tag{D.17}$$

$$K_3^H = -\lambda_3^d - \frac{\left(\left(e_{15}^I\right)^2 + C_{44}^I\varepsilon_{11}^I\right)G}{\rho} \tag{D.18}$$

Appendix E

$$\tau_{32}^{I}+i\tau_{31}^{I}=\frac{e^{-i\left(\frac{\theta}{2}+\frac{\pi}{4}\right)}}{\sqrt{2\pi r}}\frac{1}{G\sqrt{\pi a}}\left[-(\sigma_3K_1^{\tau}+q_{e0}K_2^{\tau}+q_{m0}K_3^{\tau})aRe\left[\frac{1}{\varsigma_0}\right]-\left(\lambda_4^a\sigma_3+\lambda_4^bq_{e0}+\lambda_4^dq_{m0}\right)Im\left(\frac{z_0}{\varsigma_0}\right)\right] \tag{E.1}$$

$$\tau_{32}^{II}+i\tau_{31}^{II}=\frac{e^{-i\left(\frac{\theta}{2}-\frac{\pi}{4}\right)}}{\sqrt{2\pi r}}\frac{1}{G\sqrt{a\pi}}\left[\left(\sigma_3\left(K_1^{\tau}-G\right)+q_{e0}K_2^{\tau}+q_{m0}K_3^{\tau}\right)aRe\left[\frac{1}{\varsigma_0}\right]+\left(\lambda_4^a\sigma_3+\lambda_4^bq_{e0}+\lambda_4^dq_{m0}\right)Im\left(\frac{z_0}{\varsigma_0}\right)\right] \tag{E.2}$$

$$D_2^{I}+iD_1^{I}=\frac{e^{-i\left(\frac{\theta}{2}+\frac{\pi}{4}\right)}}{\sqrt{2\pi r}}\frac{1}{G\sqrt{a\pi}}\left[-\left(\sigma_3K_1^{D}+q_{e0}K_2^{D}+q_{m0}K_3^{D}\right)aRe\left[\frac{1}{\varsigma_0}\right]-\left(\lambda_5^a\sigma_3+\lambda_5^bq_{e0}+\lambda_5^dq_{m0}\right)Im\left(\frac{z_0}{\varsigma_0}\right)\right] \tag{E.3}$$

$$D_2^{II}+iD_1^{II}=\frac{e^{-i\left(\frac{\theta}{2}-\frac{\pi}{4}\right)}}{\sqrt{2\pi r}}\frac{1}{G\sqrt{a\pi}}\left[\left(\sigma_3K_1^{D}-q_{e0}\left(G-K_2^{D}\right)+q_{m0}K_3^{D}\right)aRe\left[\frac{1}{\varsigma_0}\right]+\left(\lambda_5^a\sigma_3+\lambda_5^bq_{e0}+\lambda_5^dq_{m0}\right)Im\left(\frac{z_0}{\varsigma_0}\right)\right] \tag{E.4}$$

$$B_2^{I}+iB_1^{I}=\frac{e^{-i\left(\frac{\theta}{2}+\frac{\pi}{4}\right)}}{\sqrt{2\pi r}}\frac{1}{G\sqrt{a\pi}}\left[-\left(\sigma_3K_1^{B}+q_{e0}K_2^{B}+q_{m0}K_3^{B}\right)aRe\left(\frac{1}{\varsigma_0}\right)-\left(\lambda_6^a\sigma_3+\lambda_6^bq_{e0}+\lambda_6^dq_{m0}\right)Im\left(\frac{z_0}{\varsigma_0}\right)\right] \tag{E.5}$$

$$B_2^{II}+iB_1^{II}=\frac{e^{-i\left(\frac{\theta}{2}-\frac{\pi}{4}\right)}}{\sqrt{2\pi r}}\frac{1}{G\sqrt{a\pi}}\left[\left(\sigma_3K_1^{B}+q_{e0}K_2^{B}-q_{m0}\left(G-K_3^{B}\right)\right)aRe\left[\frac{1}{\varsigma_0}\right]+\left(\lambda_6^a\sigma_3+\lambda_6^bq_{e0}+\lambda_6^dq_{m0}\right)Im\left(\frac{z_0}{\varsigma_0}\right)\right] \tag{E.6}$$

$$\gamma_{32}^{I}+i\gamma_{31}^{I}=\frac{e^{-i\left(\frac{\theta}{2}+\frac{\pi}{4}\right)}}{\sqrt{2\pi r}}\frac{1}{G\sqrt{a\pi}}\left[-(\sigma_3\lambda_1^a+q_{e0}\lambda_2^a+q_{m0}\lambda_3^a)aRe\left(\frac{1}{\varsigma_0}\right)-(\sigma_3K_1^{\gamma}+q_{e0}K_2^{\gamma}+q_{m0}K_3^{\gamma})Im\left(\frac{z_0}{\varsigma_0}\right)\right] \tag{E.7}$$

$$\gamma_{32}^{II}+i\gamma_{31}^{II}=-\frac{e^{-i\left(\frac{\theta}{2}-\frac{\pi}{4}\right)}}{\sqrt{2\pi r}}\frac{1}{G\sqrt{a\pi}}\left[(\sigma_3\lambda_1^a+q_{e0}\lambda_2^a+q_{m0}\lambda_3^a)aRe\left[\frac{1}{\varsigma_0}\right]-(\sigma_3\lambda_1^a+q_{e0}\lambda_2^a+q_{m0}\lambda_3^a)Im\left(\frac{z_0}{\varsigma_0}\right)\right] \tag{E.8}$$

$$E_2^{I}+iE_1^{I}=-\frac{e^{-i\left(\frac{\theta}{2}+\frac{\pi}{4}\right)}}{\sqrt{2\pi r}}\frac{1}{G\sqrt{a\pi}}\left[-\left(\sigma_3\lambda_1^b+q_{e0}\lambda_2^b+q_{m0}\lambda_3^b\right)aRe\left(\frac{1}{\varsigma_0}\right)-\left(\sigma_3K_1^{E}+q_{e0}K_2^{E}+q_{m0}K_3^{E}\right)Im\left(\frac{z_0}{\varsigma_0}\right)\right] \tag{E.9}$$

$$E_2^{II}+iE_1^{II}=\frac{e^{-i\left(\frac{\theta}{2}-\frac{\pi}{4}\right)}}{\sqrt{2\pi r}}\frac{1}{G\sqrt{a\pi}}\left[\left(\sigma_3\lambda_1^b+q_{e0}\lambda_2^b+q_{m0}\lambda_3^b\right)aRe\left[\frac{1}{\varsigma_0}\right]-\left(\sigma_3\lambda_1^b+q_{e0}\lambda_2^b+q_{m0}\lambda_3^b\right)Im\left(\frac{z_0}{\varsigma_0}\right)\right] \tag{E.10}$$

$$H_2^{I}+iH_1^{I}=-\frac{e^{-i\left(\frac{\theta}{2}+\frac{\pi}{4}\right)}}{\sqrt{2\pi r}}\frac{1}{G\sqrt{a\pi}}\left[-\left(\sigma_3\lambda_1^d+q_{e0}\lambda_2^d+q_{m0}\lambda_3^d\right)aRe\left(\frac{1}{\varsigma_0}\right)-\left(\sigma_3K_1^{H}+q_{e0}K_2^{H}+q_{m0}K_3^{H}\right)Im\left(\frac{z_0}{\varsigma_0}\right)\right] \tag{E.11}$$

$$H_2^{II}+iH_1^{II}=\frac{e^{-i\left(\frac{\theta}{2}-\frac{\pi}{4}\right)}}{\sqrt{2\pi r}}\frac{1}{G\sqrt{a\pi}}\left[\left(\sigma_3\lambda_1^d+q_{e0}\lambda_2^d+q_{m0}\lambda_3^d\right)aRe\left[\frac{1}{\varsigma_0}\right]-\left(\sigma_3\lambda_1^d+q_{e0}\lambda_2^d+q_{m0}\lambda_3^d\right)Im\left(\frac{z_0}{\varsigma_0}\right)\right] \tag{E.12}$$

References

Fang, D.N., Zhang, Z.K., Soh, A.K., Lee, K.L., 2004. Fracture criteria of piezoelectric ceramics with defects. Mech. Mater. 36, 917–928.

Feng, W.J., Li, Y.S., Xu, Z.H., 2009. Transient response of an interfacial crack between dissimilar magnetoelectroelastic layers under magnetoelectromechanical impact loads: mode-I problem. Int. J. Solids Struct. 46, 3346–3356.

Feng, W.J., Su, R.K.L., Liu, J.X., Li, Y.S., 2010. Fracture analysis of bounded magnetoelectroelastic layers with interfacial cracks under magnetoelectro-mechanical loads: plane problem. J. Intell. Mater. Syst. Struct. 21, 581–594.

Feng, W., Ma, P., Pan, E., Liu, J., 2011. A magnetically impermeable and electrically permeable interface crack with a contact zone in a magnetoelectroelastic bimaterial under concentrated magnetoelectromechanical loads on the crack faces. Sci. CHINA Phys. Mech. Astron. 54, 1666–1679.

Gao, C.-F., Wang, M.-Z., 2001. General treatment of mode III interfacial crack problems in piezoelectric materials. Arch. Appl. Mech. 71, 296–306.

Gao, C.F., Tong, P., Zhang, T.Y., 2003. Interfacial crack problems in magneto-electric solids. Int. J. Eng. Sci. 41, 2105–2121.

Herrmann, K.P., Loboda, V.V., Khodanen, T.V., 2010. An interface crack with contact zones in a piezoelectric/piezomagnetic bimaterial. Arch. Appl. Mech. 80, 651–670.

Hu, K.Q., Kang, Y.L., Li, G.Q., 2006. Moving crack at the interface between two dissimilar magnetoelectroelastic materials. Acta Mech. 182, 1–16.

Li, R., Kardomateas, G.A., 2006. Mode III interface crack of piezo-electro-magneto-elastic dissimilar bi-material composites. ASME J. Appl. Mech. 73, 220–227.

Li, R., Kardomateas, G.A., 2007. The mixed mode I and II interface crack in piezoelectromagneto-elastic anisotropic bimaterials. ASME J. Appl. Mech. 74, 614–627.

Li, X.F., Liu, G.L., Lee, K.Y., 2009. Magnetoelectroelastic field induced by a crack terminating at the interface of a bi-magnetoelectric material. Philos. Mag. 89, 449–463.

Li, Y.D., Lee, K.Y., 2008. Anti-plane crack intersecting the interface in a bonded smart structure with graded magnetoelectroelastic properties. Theor. Appl. Fract. Mech. 50, 235–242.

Muskhelishvili, N.I., 1975. Some Basic Problems of the Mathematical Theory of Elasticity. Noordhoff International Publishing, Leyden.

Soh, A.K., Liu, J.X., 2004. Mode-III interface Edge crack in a magnetoelectroelastic bimaterial. Key Eng. Mater. 261–263, 393–398.

Su, R.K.L., Feng, W.J., 2008. Fracture behavior of a bonded magneto-electro-elastic rectangular plate with an interface crack. Arch. Appl. Mech. 78, 343–362.

Tian, W.Y., Gabbert, U., 2005. Parallel crack near the interface of magnetoelectroelastic bimaterials. Comput. Mater. Sci. 32, 562–576.

Wang, B.L., Mai, Y.W., 2006. Closed-form solution for an antiplane interface crack between two dissimilar magnetoelectroelastic layers. ASME J. Appl. Mech. 73, 281–290.

Wang, B.L., Han, J.C., Du, S.Y., 2010. Transient fracture of a layered magnetoelectroelastic medium. Mech. Mater. 42, 354–364.

Xiao, W., Xie, C., 2008. A technique for studying interaction between a screw dislocation dipole or a concentrated load and a mode III crack crossing an interface. Int. J. Solids Struct. 45, 5705–5715.

Zhang, T.Y., Wang, T.H., Zhao, M.H., 2002. Interaction of a piezoelectric screw dislocation with an insulating crack. Philos. Mag. A 82 (15), 2805–2824.

Zhong, X.-C., Li, X.-F., 2006. A finite length crack propagating along the interface of two dissimilar magnetoelectroelastic materials. Int. J. Eng. Sci. 44, 1394–1407.

Zhou, Z.G., Wu, L.Z., Wang, B., 2005. The dynamic behavior of two collinear interfaces cracks in magneto-electro-elastic materials. Eur. J. Mech. A/Solids 24, 253–262.